

Session MP-3

Materials/Processes(3)

Fundamental Aspects in Bumping and Via Filling Electrodeposition (*Invited*)

Kazuo KONDO, University of Okayama, Japan

Web-Based Research of Solder Paste Printing Quality

Timo RAUTAKOURA, University of Vaasa, Finland

Aulis TUOMINEN, Tampere University of Technology, Finland

Thermo-Mechanical Reliability of the Benzocyclobuten(BCB) Film in a WLCSP Process

K. O. LEE, J. YU, Korea Advanced Institute of Science and Technology, Korea

J. Y. KIM, I. S. PARK, Hynix Semiconductor Inc., Korea

The Effect of Roughness and Pattern of the Core Material to Adhesion in Making Build-up Layers

Paavo JALONEN, Aulis TUOMINEN ; Tampere University of Technology, Finland

Fundamental Aspects in Bumping and Via Filling Electrodeposition

Kazuo Kondo

Dept. of Applied Chemistry, University of Okayama

3-1-1 Tshima-Naka, Okayama 700-0082, Japan

kkondo@cc.okayama-u.ac.jp

Abstract

Foundamental aspects in bumping and via filling will be addressed. A detailed mechanism of copper via filling will be emphasised. Copper Damascene via bottom accelerating additives was investigated by patterned cathode of cathode only at via bottom. With SPS in addition to Cl, PEG and JGB, the current of via bottom cathode increases. This current also increases with an increase in SPS concentration. This accelerating effect of SPS was found with typical combination of four additives (Cl+PEG+JGB+SPS) used for via filling. The current increases with an increase in aspect ratios of patterned cathode. With higher aspect ratio of deeper via, the via bottom accelerating substance must be accumulated at via bottom. This substance is related to SPS. From the cross section observation of deposit thickness, this via bottom accelerating substance must form during electrolysis. This accumulates at via bottom of deeper via during electrolysis. SPS decomposes into monomer by electrolysis and this may accumulate and accelerates the via bottom current.

Introduction

Bumping and via filling electrodeposition became one of the most important process in recent development of electronics packaging. Especially, copper via filling has been intensively developed for damascene, build up PCB and three dimensional packaging. Micro bumping has been developed for higher pitch LCD interconnection, wafer level CSP and three dimensional packaging (Fig.1).

I started research on bumping when I was in industry since I was involved in the development of bumped type anisotropic conductive film (1). After moving to University, numerical computation of fluid dynamics within the bump cavity has been intensively studied at the diffusion controlled region. Numerical computations and experimental results coincidence have been examined for bumping with high Peclet numbers, photoresist angles, deep cavity, deep cavity for wafer level CSP (2-5).

The details of copper via filling mechanism (6,7) — inhibition and acceleration effects by additives, will be discussed in this proceeding.

Experimental

Table 1 shows the bath composition. The basic bath consists of CuSO_4 and H_2SO_4 of $0.6 \times 10^3 \text{ mol/m}^3$ and $1.85 \times 10^3 \text{ mol/m}^3$, respectively. Additives are Cl, PEG of 7500 molecular weight and JGB, whose concentrations are shown in Table 1. The baths were used for experiment more than one hour after the bath preparation.

The current-voltage curves were measured with R.D.E. with 12 mm in diameter. With potentiostatic electrolysis for the range of 100 to -400 mV vs. 3.33 mol/L KCl-AgCl, currents drop to constant value with less than three minutes.

Accordingly, all the currents were measured after three minutes from the starting of electrolysis. The R.D.E. was rotated with rotation speed of 150, 500 and 1500 r.p.m..

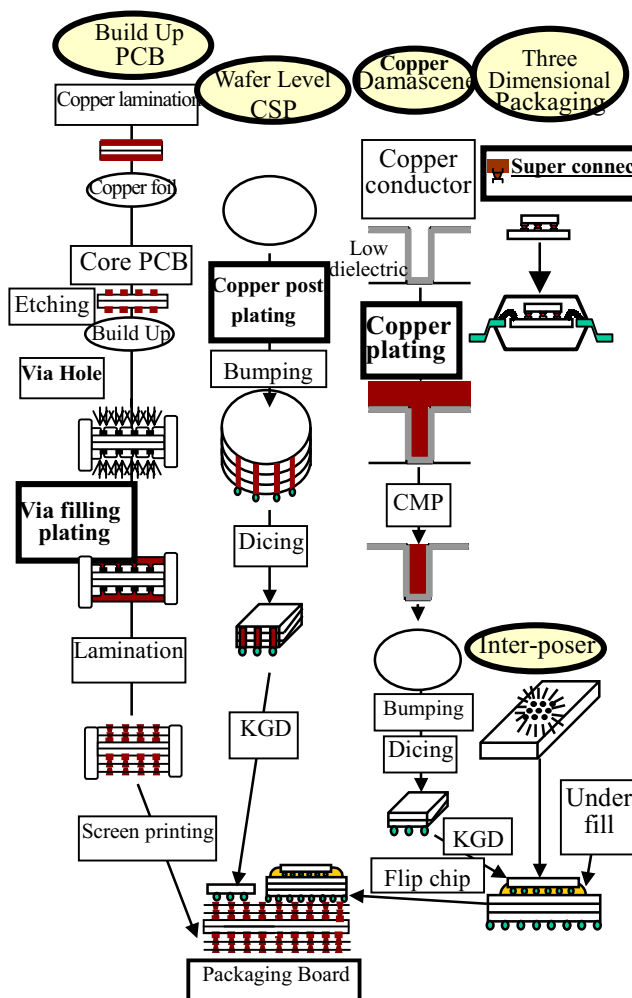


Fig.1 Recent electronics packaging process.

The patterned cathodes were prepared as follows. We formed $30 \mu\text{m}$ width and 10, 30 and $100 \mu\text{m}$ resist height pattern on copper foil. The photo resist of THB-430N (JSR Co.) was used. For 10 and $30 \mu\text{m}$ resist heights, the patterns were formed by photo lithography. $100 \mu\text{m}$ height resist was patterned by Excimer (KRF) laser with energy density of 1.0 Joul/cm^2 . The pattern has ten lines of 16 mm length with $30 \mu\text{m}$ width of 1.0 mm pitch. These photo resist patterns were attached to the rotating disk electrode (R.D.E.). The electrodeposits were prepared by constant voltage electrolysis of -200 mV vs. 3.33 mol/L KCl-AgCl without rotating the R.D.E..

Table 1 Bath composition.

Basic bath		
CuSO ₄ ·5H ₂ O		0.6 mol/L
H ₂ SO ₄		1.85 mol/L
Additive		
NaCl		100 ppm
PEG	Polyethylene glycol	400 ppm
JGB	Janus GreenB	10 ppm
SPS	Bis(3-sulfopropyl) disulfide	1, 5, 10, 20 ppm

The 30 μm width and 30 μm height resist was used for the pattern to observe the deposits cross sections. The pattern was already shown in reference 7. The electrodeposits were prepared by -300 mV vs. 3.33 mol/L KCl-AgCl without rotating the R.D.E.. 100, 200 and 400 C were applied. The deposits were then imbedded into the epoxy resin and cut and abrasive to obtain the cross sections. These cross sections were observed by optical microscopy.

Results

Current-Voltage Curves with Additives

Fig.2 is the current-voltage curves with different additives of without additive, Cl+PEG+SPS, Cl+PEG+JGB and Cl+PEG+JGB+SPS. The dotted curve is without additive.

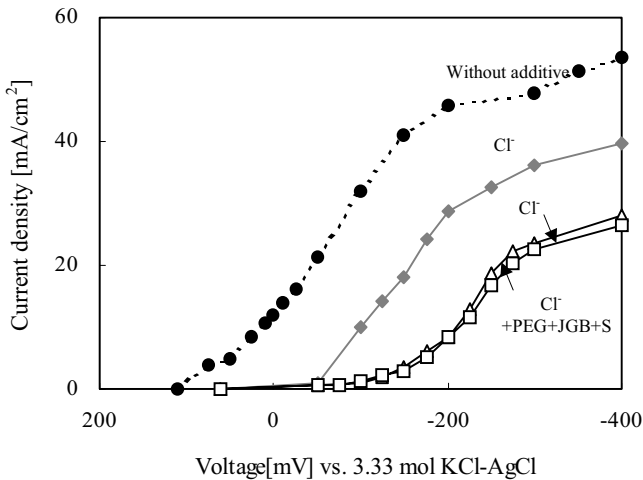


Fig.2 Effect of super-filling additives on current-voltage curves

With adding PEG and Cl, all curves shift to the cathodic side. This shift in cathodic side will be called as an inhibition effect by additives. With SPS in addition to PEG and Cl, the current increases if compared to Cl+PEG+JGB and Cl+PEG+JGB+SPS. This is due to the depolarizing effect of SPS. This depolarizing effect will be called as an acceleration effect by additives.

With SPS in addition to PEG, Cl and JGB, which is typical combination of four additives used for super via filling, however, the current does not increase. The curves with Cl+PEG+JGB+SPS and Cl+PEG+JGB are almost identical. SPS, in this case, does not seem to show the depolarizing

effect. These current-voltage curves correspond to J.Kelly's result(2,3,4).

Inhibition Effect by Additives

Fig.3(a)(b) is the current-voltage curves with different rotation speed of R.D.E. of 150, 500 and 1500 r.p.m.. The additives are Cl, PEG and JGB. With Cl and PEG of (a), current voltage curves does not shift with the rotation speed of R.D.E. With JGB in addition to Cl and PEG of (b), the curves shift to the cathodic side with an increase in rotation speed of R.D.E. such as 500 and 1500 r.p.m.. This shift in cathodic side with rotation speed means that the additives become diffusion control. Inhibition effect increases with rotation speed of R.D.E..

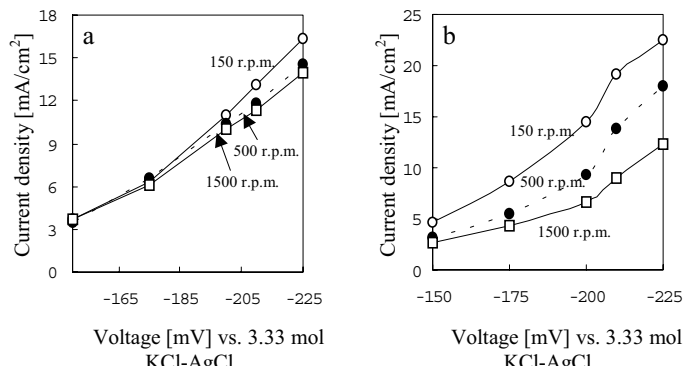


Fig.3 Effect of rotating disk speed on current-voltage curves with different additives. Additives are a) Cl and PEG, b) Cl, PEG and JGB

The adsorption of PEG molecules of about 30 nm in diameter causes this inhibition effect(7,8). The PEG molecules preferentially adsorb at the side wall of macro steps of copper electrodeposit and inhibit the lateral growth of the macro steps. Because of JGB, the PEG molecules become diffusion control. At the via outside, many PEG molecules are absorbed. Since via bottom has longer diffusion length than via outside, almost no PEG molecules can be observed at via bottom. This causes inhibition effect at the via outside and the electrodeposit preferentially fill the via bottom. This is one aspect of super via filling mechanism and this mechanism is based on the inhibition effect. Details of this diffusion control PEG molecules have already been discussed in references 7 and 8 with FESEM observations.

Acceleration Effect by Additives

We used patterned cathode of cathode only at via bottom in order to find out the acceleration effect(See Fig.4(b)). The current-voltage curves on conventional flat plate cathode have already been reported in Fig.2. Fig.4 shows a comparison of additive effect on current-voltage curves between this patterned cathode(b) and flat plate cathode(a). The additives are Cl+PEG+SPS, Cl+PEG+JGB and Cl+PEG+JGB+SPS. As have already been shown in Fig.2, the current-voltage curves with Cl+PEG+JGB and Cl+PEG+JGB+SPS are almost identical for the flat plate cathode(Fig.4(a)). With patterned cathode, these current-voltage curves are different(Fig.4(b); See white arrow). The current increases with Cl+PEG+JGB+SPS

if compared to Cl+PEG+JGB. This is because of patterned cathode. With patterned cathode, we succeeded to find the depolarizing effect of SPS with typical combination of four additives used for super via filling.

Fig.5 shows the current-voltage curves of patterned cathode with additives of Cl+PEG+JGB+SPS. The SPS concentrations have been increased from 1, 5, 10 to 20 ppm. The current increases with an increase in SPS concentration. We can conclude that SPS has depolarizing effect even with

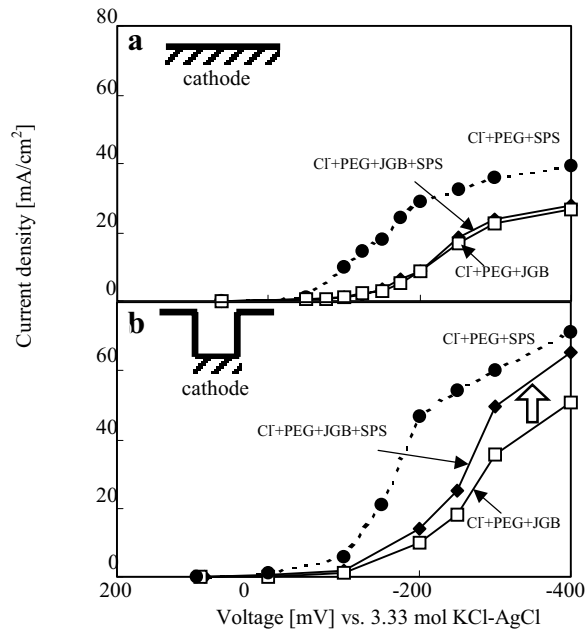


Fig.4 Current-voltage curves of flat plate cathode and patterned cathode. a) Flat plate cathode, b) Patterned cathode of cathode only at via bottom.

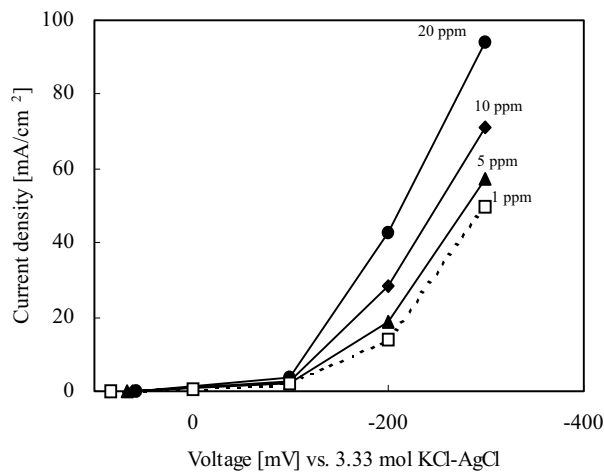


Fig.5 Current-voltage curves with different SPS concentration. Additives are Cl+PEG+JGB+SPS.

four additives of super via filling.

Fig.6 shows the current-voltage curves of different aspect ratios patterned cathodes with additives of Cl+PEG+JGB+SPS. The aspect ratios are 0.33, 1.00 and 3.33. Cathode width is fixed as 30 μm and the resist height has been changed as 10, 30 and 100 μm . The SPS concentrations are 10 and 20 ppm.

The current increases with an increase in aspect ratios of patterned cathode. The current increases with higher aspect ratio both for 10 and 20 ppm SPS concentrations.

Since the current increases with an increase in SPS

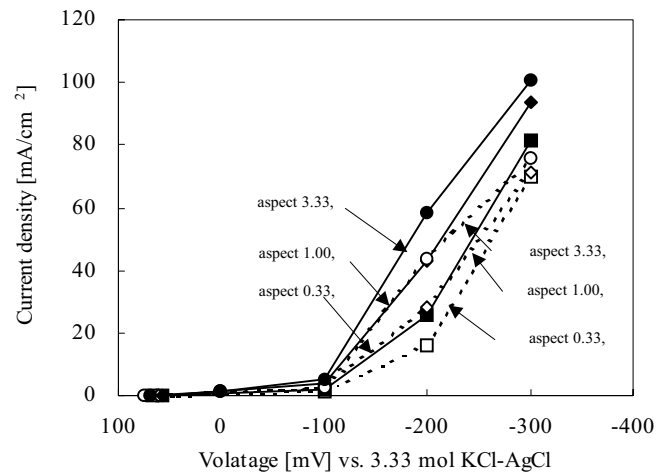


Fig.6 Effect of aspect ratio of current-voltage curves. Additives are Cl+PEG+JGB+SPS.

concentrations (Fig.5), a substance, which is related to SPS, accelerates the current of via bottom cathodes. This substance remains at via bottom since the current increases with deeper via of higher aspect ratios. This substance escapes easily from via bottom with lower aspect ratio of 0.33. The substance remains at via bottom and this accelerates the current at via bottom cathode of higher aspect ratio of 3.33.

Fig.7 is the cross section of via filling electrodeposition. The via has an aspect ratio of 1.0 of 30 μm bottom length and 30 μm resist height. Typical combination of four additives, Cl+PEG+JGB+SPS, have been used. The coulomb number has been changed from 100 C(initial stage), 200 C(middle stage) and 400 C(final stage). The lower white portion is the 30 μm in thickness copper foil and via is on the center of the copper foil. The 30 μm in thickness photo resists are on both

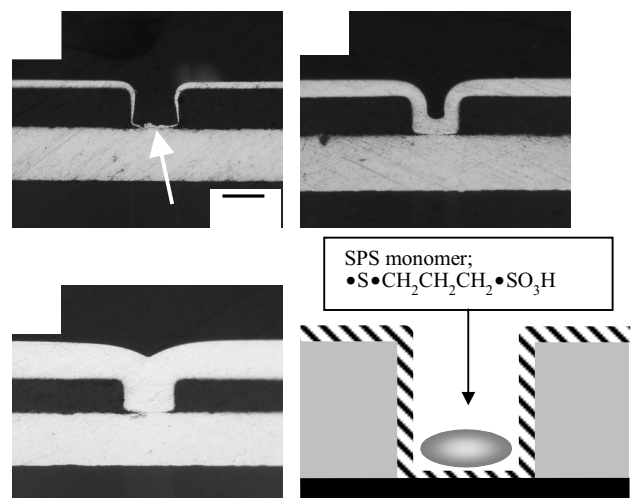


Fig.7 Cross sectional view of electrodeposit into via. a) 100 C, b) 200 C, c) 400 C, d) schematic illustration of SPS monomer.

left and right hand sides of the via. The copper electrodeposit is on the upper surfaces and sidewalls of the photo resists. The deposit is also on the copper foil via bottom.

For the initial stage (100 C) of via filling, the deposit thickness at via bottom (See arrow in Fig.7(a)) is much thinner than that at via outsides of photo resist upper surfaces. For 200 C, the via bottom thickness increases and the thickness is same for both via bottom and outsides. For the final stage of 400 C, the via bottom thickness increases drastically and the via is filled completely. At the initial stage, via bottom thickness is thinner and this thickness increases with Coulomb number. Above mentioned substance which is related to SPS is not accelerating the via bottom current at the initial stage of electrodeposition. This SPS substance starts to accelerate the current from the middle stage of electrodeposition of 200 C. The via bottom accelerating substance must forms during the electrolysis and accumulated at the via bottom of deeper via. SPS may decomposed into monomer during the electrolysis. This monomer must be the via bottom accelerating substance.

Conclusions

Copper via filling techniques are intensively developed for Damascene, build up PCB and three dimensional packaging. Micro bumping technologies is developed for higher pitch LCD interconnection and three dimensional packaging. Packaging will become as wafer level and will be involved in semiconductor fabrication process.

Electrodeposition technology has been used for packaging and PC board but now intensively penetrating into the semiconductor with copper Damascene. Dry and wet technologies are merging into the other. Electrodeposition is low cost nano meter technology and will be very intensively used for additive method forming circuits – packaging with wafer level, optical electronics and probably quantum mirage effects.

Acknowledgments

Thanks so much for NEDO and ASET for financing via filling project.

References

- 1.K. Kondo et al., Proc. in 8th Euro. Hybrid Microel. Conf.,Rotteldam (1991)
2. K. Kondo et al., JES,144(1997)466
3. K. Kondo et al., JES,145 (1998)840
4. K. Kondo et al., JES,145(1998)3007
5. K. Kondo et al., JIEP,2,1,p35,(1999)
6. K. Kondo et al., JIEP, 3,607-612(2000)
7. K. Kondo et al., ECS-ISTC2000,Shanghai,May, (2001)

Thermo-Mechanical Reliability of the Benzocyclobuten(BCB) film in a WLCSP process

K. O. Lee¹, Jin Yu¹, J. Y. Kim² and I.S Park²

¹Center for Electronic Packaging Materials

Dept. of Materials Science & Engineering, Korea Advanced Institute of Science and Technology,

373-1 Kusong-dong, Yusong-gu, Daejeon, 305-701, S. Korea

e-mail) sam813@cais.kaist.ac.kr jinyu@cais.kaist.ac.kr

²Advanced package development team, Package & Module R & D Center, Hynix Semiconductor Inc.

e-mail) kimjy@hynix.com pisa@hynix.com

Abstract

A new WLCSP process which enables reliable fabrication of high-performance and low cost package has been developed based on the low dielectric passivation layer. The fabrication process can be reduced by using the newly developed photosensitive-BCB and a conventional photolithography process. However, cracks frequently nucleating on the BCB poses serious reliability issues.

In order to prevent the crack generation, the stresses in the BCB layer were reduced by optimizing the relative thickness of the BCB and the underlying stress buffer layer(SBL), and by stabilizing the BCB microstructure with optimal photo lithography processes. The microstructure of the BCB was investigated by measuring the molecular weight, the cross link element intensity and the glass transition temperature.

Introduction

Wafer level chip scale package(WLCSP) has major economic advantages over the conventional process by packaging and testing before the wafer dicing.[1]

Various polymers have been used as dielectric layers [2], and among them benzocyclobuten(BCB) is used as a high density interconnect dielectric material because of the high glass transition temperature(Tg), low dielectric constant and low water absorption. [3] The polymerizaion of functional monomers of BCB is a thermal process which does neither require catalysts nor generate volatile by-products. However, being a thermosetting polymer, BCB consists of such rigid functional groups as benzene rings which it can be easily broken during the thermal cycling test. Therefore, a key requirement of BCB used in WLCSP is the thermo-mechanical reliability. Methods to enhance the thermo-mechanical reliability include the reduction of stresses in the BCB layer by optimizing the thickness of BCB and the underlying stress buffer layer(SBL), and the modification of the BCB microstructure with the strong crack resistance by optimizing the curing condition.

Experimental procedure

CYCLOTENETM 4024, a photosensitive polymer developed by DOW Chemical, was used as the solder mask material, an the BCB resins are supplied as solutions of B-staged monomers in mesitylene. Mechanical properties of used SBL and BCB are shown in Table 1. [4]

Materials	SBL	BCB
CTE(ppm/°C)	190	52
Young's Modulus(GPa)	0.34	2.9 ± 0.2
Ultimate Tensile Strength(MPa)		87 ± 9
Rupture Strain		8 ± 2.5

Table 1. Mechanical properties of the SBL and BCB

Figure 1 shows a schematic diagram of the wafer-level CSP of the 72M Rambus DRAM by Hynix Ltd. [5] A

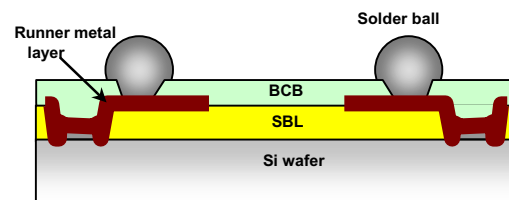


Figure 1 A schematic diagram of WLCSP by Hynix Ltd.

dielectric polymer of 20-30 μm thick was spin coated over the Si wafer as the SBL to relax the thermal stress. The SBL material used in this study consisted of modified polyimide prepreg with n-Methyl pyrrolidione(NMP) solvent, which

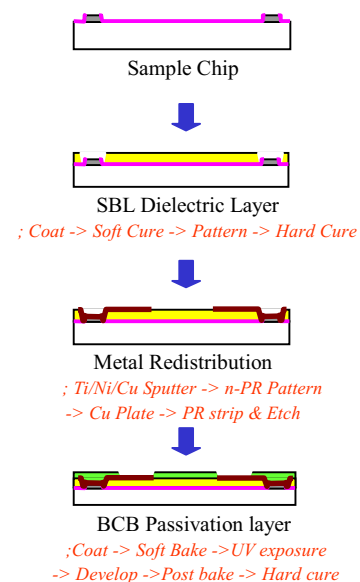


Figure 2 Fabrication process flow of WLCSP.

has a high CTE/modulus compared to the conventional

dielectric polymer, good moisture resistance and low dielectric constant. The package provided redistributions from the peripheral bond pads of existing IC design to the area arrays of I/O bumps, which was made by the sputtering and electroplating of the runner metal layer. Here, the runner metal consisted of Ti/Ni/Cu. The BCB layer at the top

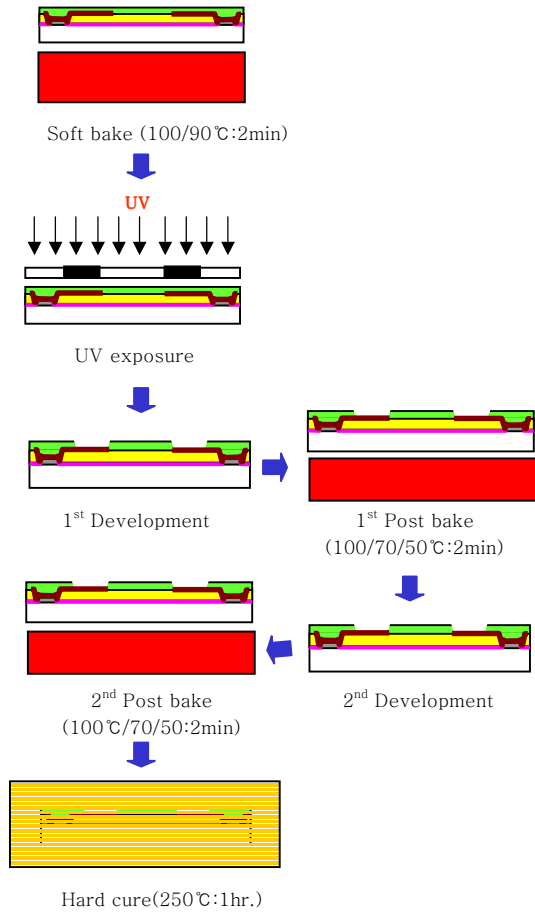


Figure 3 BCB Lithography Process

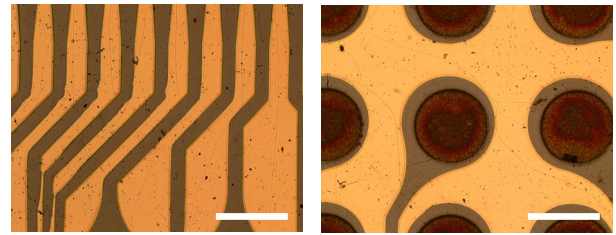
protected the metal line and defined the solder ball pad. The whole fabrication process of making the package is shown in the Fig.2.[6]

Among the processes listed, only the BCB photolithography processes were varied to give different BCB microstructure. Figure 3 shows the BCB lithography process in detail. After the BCB resins were spin coated over the runner metal redistributed layer to the thickness of 10-20 μm , substrates were soft cured at 90°C or 100°C for 2 minutes, which were followed by the UV exposure. The BCB development was conducted in two steps due to the thickness of the layer, and the substrates were post baked for 2 minutes at either 50°C, 70°C, or 100°C. After the 2nd development and 2nd post baking at the same temperature as the 1st post bake temperature, substrates were hard cured at 250°C in vacuum furnace for 1 hour, and the patterned BCB/runner metal/SBL/Si substrates without the solder ball attachment were subjected to the thermal cycling tests in the temperature range of -65~150°C.

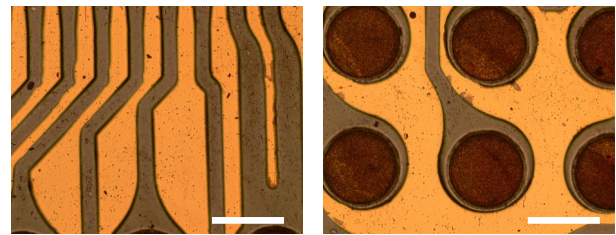
The molecular weight of BCB was measured using the gel permeation chromatography(GPC), and the density of cyclobuten parts of the BCB monomer was measured using the nuclear magnetic resonance(NMR). The glass transition temperature of the BCB was measured using the differential scanning calorimeter(DSC).

Results and Discussions

The bi-axial stress in the BCB layer during the thermal cycle was calculated by using an elementary beam analysis of the simplified Si/SBL/BCB layers, and the stress in the BCB was 69Mpa, which varied less than 1% with the BCB or SBL thickness. Figure 4 shows optical images of specimens after



(a) After 100cycles [SBL 20 μm - BCB 10 μm]



(b) After 700cycles [SBL 30 μm - BCB 20 μm]

Figure 4. The thermal cycle result of patterning structure with respect to the SBL and BCB thickness

thermally cycling, which were soft baked and 1st post baked all at 100°C. The crack resistance tended to increase slightly with the thickness of the BCB and SBL layers, but all the specimens did not pass 1000cycles, suggesting that the crack

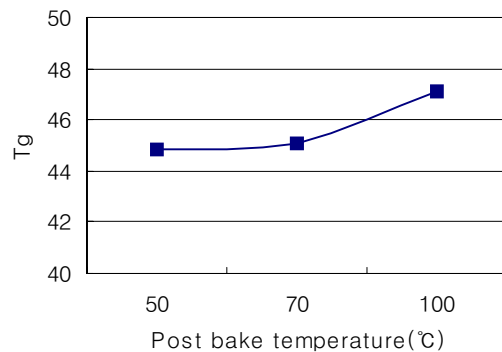
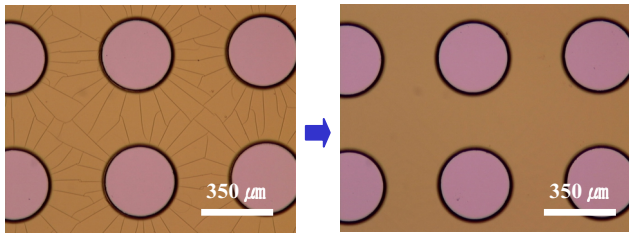


Figure 5. The glass transition temperature(T_g) with respect to the 1st post bake temperature

generation can not be prevented by the thickness variation alone.

The glass transition temperatures (T_g) of the BCB polymers soft cured at 100°C were measured using DSC and presented in Fig.5. It can be seen that variations of the 1st post bake temperature did not affect T_g much, which ranged between $45\sim 50^\circ\text{C}$. In general, when the specimens not fully polymerized, suffer larger stress below the glass transition temperature, cracking can occur [7]. Thus, cracks seemed to have occurred during the 2nd development process (at R.T) right after the 1st post baking, in the present case. The point is shown in Fig.6, which shows clearly that BCB cracks were formed during the 2nd development process. However, specimens which were post baked at 50°C or 70°C , and 2nd developed at R.T did not show BCB cracking. Therefore, it appears that cracks are generated more easily at the 2nd



(a) Right after 2nd development (b) Right after 2nd post bake at 100°C

Figure 6 The optical image of the top view of BCB

develop stage when the specimens were 1st post baked at higher temperature.

It can be seen from Fig. 6 (b) that cracks formed at the 2nd development stage were healed during the following 2nd post bake temperature at 100°C .

Variations of the molecular weight of BCB right after the 2nd post baking treatment as function of the soft bake or post

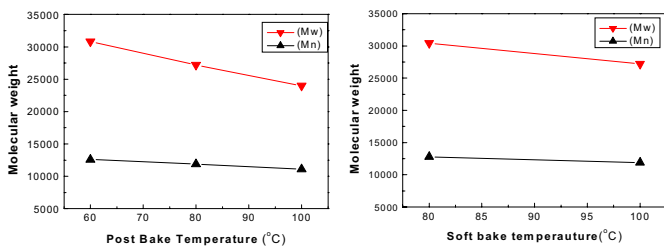


Figure 7. The molecular weight change with respect to the soft bake temperature and post bake temperature

(Mw: The weight average molecular weight
Mn: The number average molecular weight)

bake temperatures are shown in Fig.7. Note that the molecular weight of BCB decreased with the soft and post bake temperatures, which affected the final molecular structure and ultimately the thermo-mechanical property of BCB.

The proton intensity of the cyclobuten parts and the vinyl parts of the BCB monomer measured by NMR is normalized with respect to the proton intensity of the phenyl parts, and presented as a function of the post bake temperature in

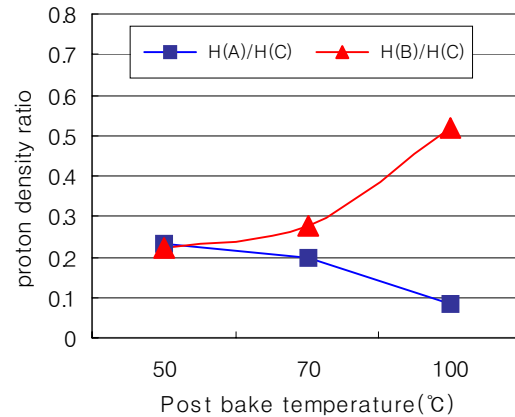
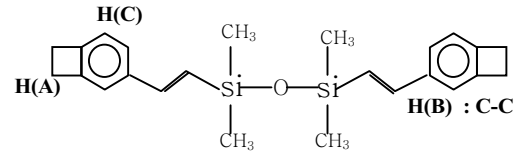
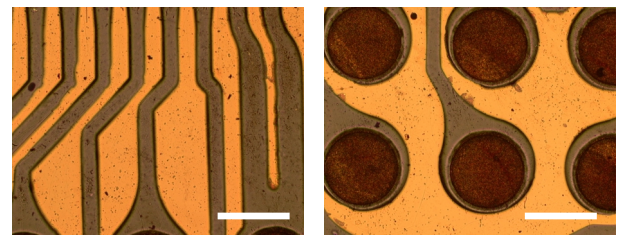
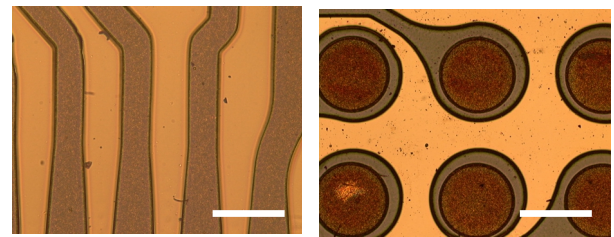


Figure 8 The proton density ratio of cyclobuten proton to phenyl proton ($H(A)/H(C)$) and vinyl proton to phenyl proton ($H(B)/H(C)$) with respect to the post bake temperature

Fig.8. Note that the proton intensity of the cyclobuten parts decreased, and the proton intensity of the vinyl parts increased with post bake temperature. Thus, fewer cyclobuten parts were remained at higher post bake temperature, and this exacerbate the propensity of cracking because cyclobuten parts linked with the $\text{C}=\text{C}$ double bonds of another BCB monomer at the hard cure stage at 250°C are known to form



(a) After 500cycles [soft bake(100°C) – post bake(100°C)]



(b) After 1000cycles [soft bake(90°C) - Post bake(50°C)]

Figure 9. The thermal cycle test result of patterned structure with varying the soft bake temperature and 1st post bake temperature

stable molecular structure

Optical images of patterned WLCSB with $30\ \mu\text{m}$ thick SBL and $20\ \mu\text{m}$ thick BCB after the thermal cycling test are presented in Fig.9. Here, specimens soft and post baked at lower temperature showed better crack resistance of BCB,

and the specimens which were soft and post baked at 90°C and 50°C, respectively, did not show any surface crack in the BCB layer.

Conclusions

Increasing the thickness of the BCB or SBL layer was not effective to prevent cracking in the BCB layer. However, modification of the BCB microstructure by reducing the soft and post bake temperatures seemed to contribute to the thermo-mechanical stability. The BCB cracking could be prevented by lowering the soft and post bake temperatures to 90 and 50°C, respectively.

Acknowledgments

This work was supported by the Center for Electronic Packing Materials(CEPM) which is an engineering research center funded by Korea Science and Engineering Foundation(KOSEF)

References

1. J.Simon, M. Topper, H. Reichl, and G. Chmiel, Proceedings of the International Flip Chip, Ball Grid Array, TAB and Advanced Packaging Symposium, pp 13-16(1996)
2. H.B.Bakoglu, Circuits, Interconnections, and Packaging for VLSI, p.81, Addison Wesley(1989)
3. R. W. Jonson, T.L. Phillips, W.K. Weidner, S.F.Hahn, D.C. Burdeaux and P.H. Townsend, IEEE Trans. CHMT 13, 347(1990)
4. Jang-hi Im, Edward O. Shaffer II. et al, Journal of Electronic Packaging, vol.122, p.28-33 (2000)
5. In-Soo Kang, Jong-Heon Kim, I.S Park, Ki-Rok Hur and Soon-Jin Cho, Electronic Components and Technology Conference, pp 87-92 (2000)
6. Andrew J.G. Strandjord, Daniel M. Schock, and Scott R.Kisting, The international journal of Microcircuits and Electronic Packaging, vol 19, pp 260-280 (1996)
7. Rudolph D. Deanin, Polymer structure, properties and applications , Cahners books(Massachusetts, (1972), pp. 153-161.

Web-Based Research of Solder Paste Printing Quality

Timo Rautakoura

Dept. of Information Technology and Production Economics, University of Vaasa

P.O. Box 700, FIN-65101 Vaasa, Finland

Email tirauta@uwasa.fi,

Tel. 358 6 324 8111

Fax 358 6 324 8725

Aulis Tuominen

Pori School of Technology and Economics, Tampere University of Technology

P.O. Box 300, FIN-28101 Pori, Finland

Email aulis.tuominen@pori.tut.fi

Tel 358 2 627 2700

Abstract

This paper outlines a way to operate solder paste quality control system using WWW-based technology in the context of researching paste parameters and to find out the most effective set of printing parameters to obtain enough reliable solder paste printing. User of the system should have possibilities to choose different parameters and examine their influences on the measuring process. System could also be used in context of a virtual studying and training. In addition to paste measurement the proposed system could applied to other similar industrial measurement problems.

Introduction

Electronic products are changing rapidly and their lifespan is coming shorter and shorter. Competition in electronics production is hard – price is not anymore a competitive advantage. The most important ways to compete, in addition to effective marketing and logistics, are high-quality products and efficient production, which can be achieved by product and production development. According to Danielson [1] controlling the process of production is the most important factor affecting competitiveness in electronics industry. Better product can bring in better coverage and effective production may lower the costs. However, competitors quickly catch the lead and that is why companies have to develop all these sectors constantly.

There is a need to get new products as quickly as possible to the market. This means that the time spent in product development is often short. Also, a big amount of products is brought to the market. The rapid development of products and production methods sets always new challenges for the production process. Often the problems that appear are such that previous knowledge cannot be fully exploited. However, the production lines must be made working with full capacity as soon as possible and the products must be of the highest quality. The company that gets its products to the market first, gets the best coverage and often the position as a market leader. The thing that matters is the quality. Bad quality causes the need for corrections which can often be costly. The bad quality also harms the reputation of the company as a reliable producer.

Solder Paste Quality

More than half of solder faults in electronics production arise in solder paste printing [2]. However, it is fairly cheap to correct these mistakes. When discarding a faulty product only couple of tens of seconds is lost and also the losses of material are relatively small. Faulty circuit board are easy to wash or they can be removed from the production line when there is only the loss of material: paste and washing liquid or a circuit board.

On fast production lines visual inspection of paste printing quality is both unreliable and slow. Slowness is a problem also in controlling which is based on utilizing machine vision - that is why controlling is based on statistical observations and only the most problematic things are controlled. In controlling based on statistics the development of forecasting parameter is examined. In this way the mistake can be expected and corrections in the process can be made before the actual mistake appears.

There have been several studies on the solder printing parameters and inspection [3], [4], [5], [6], [7], [8] although the large number of parameters influencing to the printing results makes finding the mistakes difficult, and probably all parameters are not even known yet. The large number of parameters and the problems they cause complicates also the development of paste printing simulation models. If it could be possible to model the paste printing, the empirical research could be partly replaced by simulations. At the moment the impact of unknown factors has to be examined empirically and experimentally.

The traditional way of testing has been to vary the values of parameters empirically until the accepted result is reached. In these cases the printing results are usually evaluated approximately and the analysis of the reasons influencing the final results is mainly based on experience or, in the worst case, on vague guessing. Defining the problem systematically needs lots of experimenting and extensive material of test results as well as analyzing the complicated relations between causes and consequences.

Experimental research can be made faster by automating the measuring and decision-making. Checking if the paste is placed properly is fairly easy by using 2D-machine-vision-system. There are also several commercial solutions for this task but for measuring and analyze fast enough and reliable the volume of the paste only few systems exist.

To find out printing parameters experimentally needs only to check the places, where the errors are supposed to exist. Typical places are very small paste spots and those, which are very close each other.

Computers fast function and ability to control big amount of data makes it possible to automate decision making for instance by means of statistics or Soft Computing or to combine these to human knowledge.

Remote Control

Outsourcing the production brings product development and manufacturing apart. Many small EMC-companies (Electronic Manufacturing Service) do not have resources or possibilities to invest in research of electronics production methods due to relative unstable relationships with customers. Because of the security policy the research and development facilities of big companies may not be available either. One possibility is to co-operate in research, prototyping and training with an independent research institute. This kind of an institute could be for example a university or a research laboratory. Also some companies could provide their resources to be used for reseach purposes.

The co-operation could be carried out by utilizing the possibilities of the Internet. Internet- and WWW-based process control systems are already generally available. Also many laboratory [9], [10], [11] and even commercial solutions exist to operate devices remotely [12]. There are also many solutions for educational purposes which are used via Internet [13], [14], [15]. The problem does not seem to be the availability of solutions but inadequate security and unreliable data transmission. Also non-standardized protocols make it difficult to operate in Internet.

Usually every supplier has its own protocol to handle the data transmission between the equipment and solutions. To use the same supplier for all equipment is problematic. But also using other supplier and their equipment which have a different way to communicate leads to problems. This is problematic because there is a need for two programs between each device and application, which translate the communication protocol for them, one on each direction. Fig. 1 represents the guidelines for communication between several equipment and application and transforming communication between each one.

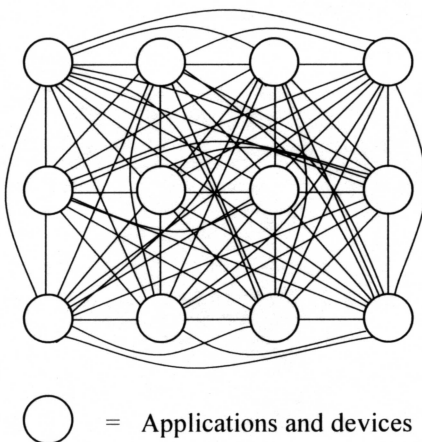


Fig 1. Each application and device has its own protocol

In this case it is quite expensive and difficult to install new devices and fit all to each other.

Another solution is to use universal communication standards or transformation program between equipment. However, agreeing upon the standardation could be difficult – every supplier would like to have his protocol as the standard. OPC (Ole Process Control), which is based on Microsoft OLE-technology, was primarily developed for communication between automation equipment but it is now developed also for communication between equipment and applications. OPC serves as a common interface between equipment and applications which have their own protocols. Thus there is no need for standardization. The only transformation program is the communication with OPC. This simplifies the communication between any solution, every supplier only needs to adapt their architecture according to a common interface [16].

Fig. 2 represents the guidelines for communication between several equipment and application using OPC. In this case the protocol structure is very simple.

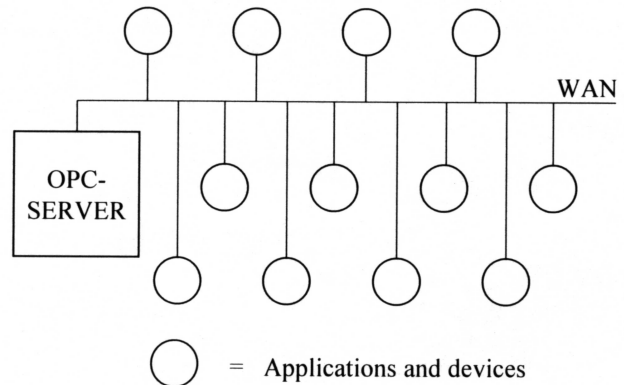


Fig 2. Applications and devices use OPC-protocol

Using and controlling equipment and application via Internet is based on dynamic inquiry. When clicking a cell in WWW-page the application sends a message to a server which the device or application is connected to. Application in server starts a small program, which reads the message and it can read or load the states in register of the device. Then the device does the operations, which state is in its registers. In case of reading the state, the program sends the register value to other application or back to the WWW-page in certain cell.

The slow and unreliable data transfer makes the Internet unsuitable for solution, which are time-critical or need high reliability. However, the data transfer speed and reliability improves all the time. To create an Intranet between client and service it is easier to control reliability and to reserve enough data transfer bandwidth. Fast technology development makes it near future possible to do even critical operations via Internet. And this is already possible today's technology. For example, September 2001 an operation was made remotely: Doctors who were in United States did a surgical operation to the patient who was in France. Doctors watch the operation on

real time video and controlled robot hands, which removed patients gallbladder. The connection was fiberoptic high-bandwidth point-to-point connection and the delay time was only 150 milliseconds (17).

Outline of Solder Paste Research system

In the next sections is described an outline of a solder paste printing research and quality control system, which can be used via Internet. There is also explained the function of the system and the advantages that can be achieved with it. The equipment can be used via Internet, Intranet, and Extranet and on site. The proposed system is tested in a simplified laboratory surrounding.

Structure of the system

In figure 3 shows a diagram of the structure of the research environment and its Internet connection. Circuit boards which are going to be examined are loaded to circuit board rack (1). Paste printing machinery (2) is equipped with a fast and accurate video camera (9) which follows the squeegee. In the front of the printed circuit boards inspection device (4) is a buffering board rack. (3). Printed circuit board inspection device includes a camera system (10), which inspects locations and volumes of the critical paste spots. Inspected circuit boards go to a circuit board rack (5), where they can be stored for later inspection. Printed and inspected circuit boards can be recycled back to board rack (1) through the washing and drying device (6).

The equipment includes OPC-server (11), which controls the messages from other devices and applications. Messages which come from outside of the local area network, need an Internet-connection. Also The WWW-server with necessary interface (control board and screen or a Virtual Reality equipment) (7. 8) is required.

Operation of the system

When researcher wants to use the research equipment he looks for the next vacant time on WWW-site and reserves the needed hours. Before to start using the equipment sufficient amount of printing boards have to be sent to research laboratory. Laboratory needs also a stencil or the stencil can be made in laboratory according to the circuit board CAD data. Laboratory may already have some boards and stencils used often. Researcher also needs to check that the needed paste material is available in the laboratory.

Before to start using the research equipment the needed amount of printing boards have to be loaded into the printing board rack. The research can be done with only one board, which is recycled to start after measuring and cleaning. This takes more time and minimum amount is about 6 to 10 if the boards need not to be saved and removed from the line for later inspection. The environmental conditions, like temperature and humidity as well as the temperature and viscosity of the paste need to stabilize before starting. Researcher can define printing parameters for speed, pressure and the angle of squeegee according to his own experience. One or the all parameters can be also left for the program of the system to choose. The parameters, chosen by the system can be based on the results of similar printing conditions and layouts. All data from parameters and environmental conditions is saved in database to the connection of identification data of the printing board.

Researcher fills in the required data to the cells of the WWW-page (Fig. 4). Data is then sent to the server of the research system which adapts the data to the receiving applications or devices.

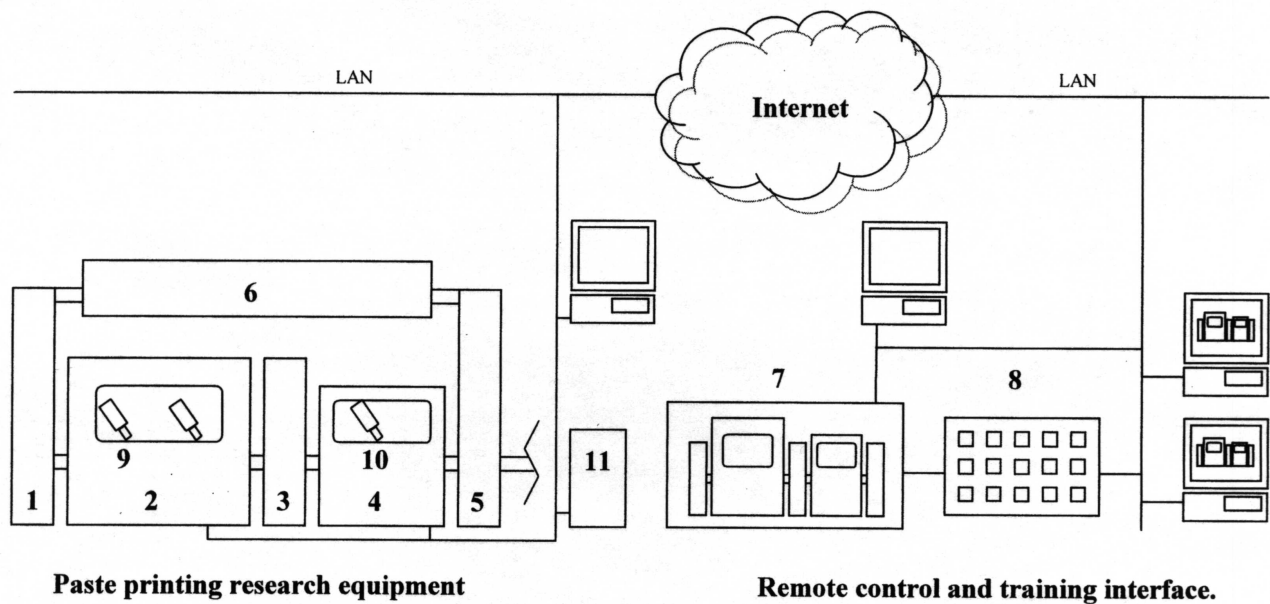


Fig 3. The diagram of solder paste research equipment

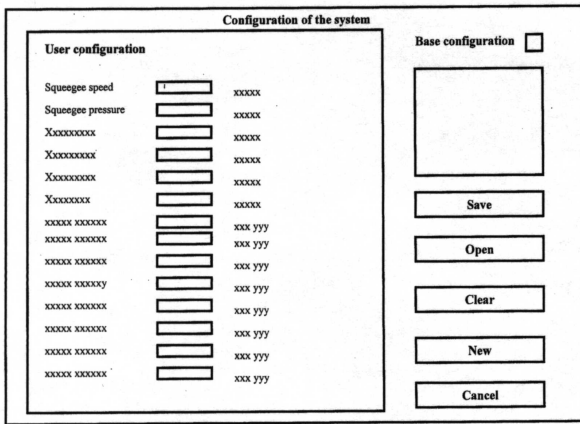


Fig. 4. Example of an input page

Operation of the system is controlled with normal computer machinery and WWW-browser. Researcher fills in the data to cells on WWW-page and there may also be simulated control panel on the screen. Receiving data is also seen on the same screen. System interface can be developed to feel more real. When using for studying and training purposes the small computer screen can be replaced by large 3D-panel, where the operator can be "inside". Screen can also be replaced by "data-glasses" to where the data and video is delivered.

Fast and accurate video camera takes pictures from printing process. The camera follows the squeegee and the target of the picture can be changed along the squeegee. If the researcher wants to examine the printing process more carefully it is possible by loading a saved video to ones own computer and examine it later. After the printing process another camera system takes a picture of a stencil. From the picture of paste sticking it is possible to draw a conclusions of need for stencils cleaning. Picture is also used to decide, which areas are critical and need to be measured in volume inspection.

Volume control system takes pictures with several fast and accurate cameras. Each camera sweeps a narrow strip over the printed board. System takes pictures of predetermined areas and the areas which the decision of stencil inspection leads in. Camera system processes from the picture data only the exact spot, where the solder exists. This is known from stencils and PCBs CAD-data. After processing the data is sent to computer system which analyses the results and compares them to target values. Data of paste spots, which are between accepted limits, is not saved. System creates a three-dimensional volume model of the spots, which exceed the accepted limits. Geometrical data is then saved in the database with location- and identification information. The system shows the faulty spots on a picture of printed board (Fig. 5). The researcher can then choose some spot to examine them closer. If so the system sends to researcher the accurate geometrical and identification data of the spot. The data can be user to create a wireframe and rendered model of paste spot (Fig 6.).

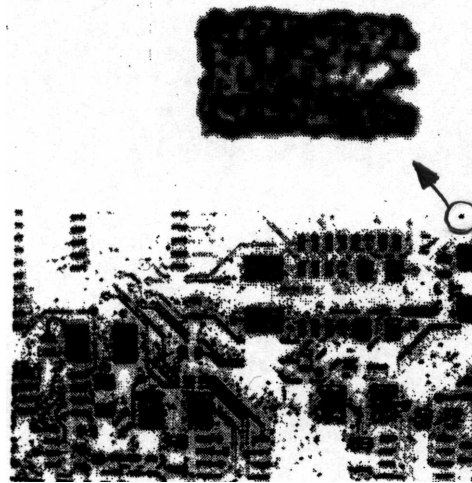


Fig. 5. The faulty solder spot on the board

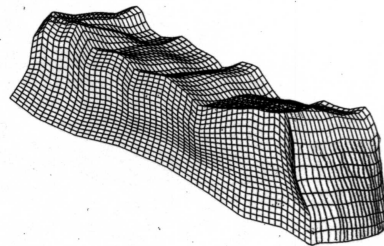


Fig 6. Wire frame model

Researcher can take any circuit board off the line to other buffer rack when there is need for closer inspection. This board can any time take back to line and make additional measurements by inspection camera system from the required spots or areas. Circuit boards, which are not needed to examine later go to the end rack. They return back to beginning through the cleaning and drying device. When needed, printed and accepted circuit boards may be steered forward on the line to the next production process.

System analyses the inspected boards and when needed it changes the printing parameter set to next printing event. System can also change the printing parameters to examine other cases. Also researcher can choose the new parameter set. To choose parameters automatically it is possible to search the acceptable result continuing drive and it produces a lot of data to statistical analyse.

Benefits of using the system

With this system it is possible to get varied range of research material, which can be used to solve the paste printing parameters. Researched material is also useful, when there is a need to develop a paste printing modelling. The system gives accurate and exact information of the volume and shape of solder spots instead of rough "accepted or rejected" result. The information is useful also for examining and analysing the printing processeven better. It is possible to steer the resources even more effectively if the research activities are concentrated into a specialized laboratory.

Automated equipment is available via Internet all over the world 24 hours a day.

Conclusions

In this paper it is explained an outline of the construction of paste printing research system, its functions and the way how to use it via Internet worldwide. This example is of paste printing but the concept is the same for other processes in electronics manufacturing.

Both to small and big manufacturers and EMS-companies the WWW-based research system offers a possibility to use a modern research technology and apply latest research to their own work. They can do pre-research and examinations in the beginning and during the research and development activities as well as when a new product or production line is launched. The research system helps minimize the ramp-up-time and when a new product comes to production the production line can immediately start running at full capacity. Companies can also outsource some of the research and development activities, which help them to concentrate on their core businesses.

Some research institutes may specialize in certain research area in electronics manufacturing. In order to establish networking with the each other they can offer research, product and production development, testing and training services and even co-operate in launching new products. The concept is possible to apply to all same kind of technical processes and it is possible to use the described system between universities to implement virtual training and studying methods. The method makes it possible to substitute a part or all expensive laboratory work with simulated or virtual distance working. This makes it also possible to use laboratory work in the context of theoretical material, which leads studying to real Problem Based Learning.

The most significant weaknesses of the proposed system are slow Internet connections and the lack of fast enough and accurate paste inspection device. There are available some commercial solutions which are good enough for pilot work purposes but the tremendous amount of raw data they produce should be much smaller to transfer and analyse data faster. The results we have got when using and testing the proposed system encourage us continue the research work further. The speed and other properties of data transfer in Internet develops all the time, which make it possible to transfer more data at higher speed.

References

1. Danielsson, H., Surface Mount Technology With Fine Pitch Components, Chapman & Hall (1995), p. 1.
2. Buttars, S. P., "Parameters for Solder Paste Printing for Fine Pitch Components," Proc NEPCON West '93, Anaheim, Cal, Vol 3, 1993.
3. Jianbiao, P., Tonkay, G. L., Storer, R. H. Sallade, R. M., Leandri, D. J., "Critical variables of solder paste stencil printing for micro-PGA and fine pitch QFP," *Electronic Manufacturing Technology Symposium 1999, Twenty-Fourth IEEE/CPMT, 1999.*
4. Nguty, T. A., Riedlin, M. H. A., Ekere, N. N., "Evaluation of Process Parameters for Flip Chip Stencil Printing," *Electronics Manufacturing Technology Symposium, 1998 Twenty-Third IEEE/CPMT, 1998.*
5. Tonapi, S. S., Srihari, K., Testani, M., Serafini, J. and Ferrano, S., "Implementation of the Pin-In-Paste Process In a Contract Manufacturing Environment," *The 15th International Conference on Production Research 1999, pp. 1211-1214.*
6. Ekere, N. N., Mannan, S. H., Currie, M. A., "Solder paste printing process modeling map," *Electronic Manufacturing Technology Symposium. Proceedings of Japan International, 18th IEEE/CPMT International. 1995, pp. 137-141.*
7. Okura, T., Kanai, M. Ogata, S., Takei, T., Takakusagi, H., "Optimization of solder paste printability with laser inspection technique," *Electronics Manufacturing Technology Symposium, Manufacturing Technologies – Present and Future, Seventeenth IEEE/CPMT International. 1995, pp. 361-365.*
8. Venkateswaran, S. Srirani, K., Adriane, J. H., Westby, G. R., "A realtime process control system for solder paste stencil printing," *Electronics Manufacturing Technology Symposium, 1997 Twenty-First IEEE/CPMT, 1997.*
9. Massachusetts Institute of Technology, <http://web.mit.edu/hmsl/www/Telesurgery/> (25.9.2001).
10. Taylor, K., Dalton, B. "Issues in Internet Telerobotics," *FSR'97 International Conference on Field and Service Canberra, Australia, 1997.*
11. Milgram, P., Rastogi, A., Grodski, J., "Telerobotic Control Using Augmented Reality," *Proceedings 4TH IEEE International Workshop on Robot and Human Communication (RO-MAN'95), Tokyo 1995.*
12. National Instruments, <http://www.ni.com/> (14.9.2001).
13. Tilbury, D., Luntz, J, Messner W., "Control education on the WWW: tutorials for MATLAB and SIMULINK," *American Control Conference, Proceedings of the 1998.*
14. Paulos, E., Canny, J., "Delivering real reality to the World Wide Web via telerobotics," *Robotics and Automation, Proceedings IEEE International, 1996.*
15. Tillbury, D., Messner W. C., "Control Tutorials for Software Instruction over the word wide Web," *IEEE transactions on education, Vol. 42, No. 4, November 1999.*
16. OPC-Foundation. <http://www.opcfoundation.com>. (18.9.2001).
17. Computerworld News September 26, "High-speed telecom services make trans-Atlantic surgery possible," http://www.computerworld.com/storyba/0,4125,NAV47_S TO64256,00.html (28.9.2001).

A study on the nucleation behavior of zinc particles on aluminum substrate

Sung-Ki Lee, Jeong-Gi Jin, Young-Ho Kim, Jae-Ho Lee*

Dept. of Materials Engineering, Hanyang Univ., Seoul, 133-791, Korea

*Dept. of Met. Engr. & Mat. Sci, Hongik Univ., Seoul, 121-791, Korea

E-mail: package@empal.com, Phone: 82-2-2290-0405, Fax: 82-2-2293-7445

Abstract

The nucleation and growth behavior of zinc particles deposited from the zincate solution on aluminum substrates were investigated. The zinc particles initially nucleated on the peak or edge of the aluminum surface where was exposed to the zincate solution, and preferentially grew with {0001} plane of hexagonal platelets. In case of zincate treatment on Al alloy substrate, substrate is fully covered by a thin layer of small zinc particles. At high temperature, zinc particles grew with [1100]-oriented hexagonal structure and were appeared a starfish-like shape like the coalescence of hexagonal structure.

Introduction

The flip-chip technology gained an important role in electronic assembly. An increasing number of products contain flip-chip due to size reduction, increase electrical performance and cost saving potential. [10] This flip chip process employs solder bump to electrically and mechanically connect an integrated circuit device to a substrate in a facedown configuration. Manufacturing of solder bumps on aluminum pads needs to introduce an intermediate layer to avoid the direct interaction between aluminum and the solder contents. The solder bumps are usually deposited onto the chip terminal pads, which are coated with an interface or under bump metallurgy (UBM). One of the major functions of the UBM is to promote and maintain adhesion of the solder bumps to the underlying aluminum terminal pads. Many different methods have been employed to fabricate the UBM and solder bumps, including conventional sputtering, evaporation and electroplating techniques. Among these studies, electroless plating has the highest potential for cost reduction of the bumping process in flip chip applications. It provides a selective autocatalytic metal deposition directly on the aluminum pads, and therefore lithography and etching processes are not required. However, due to the high affinity of aluminum to oxygen, aluminum pads exposed to air or to aqueous solution are always covered with thin layer of aluminum oxide or hydroxide. [1] Zincate treatment of aluminum pads is an essential step to make aluminum pads actives for subsequent electroless nickel plating. Major aims of the zincate treatment are to provide an intermediate layer that can initiate electroless nickel deposition. It was recognized that morphology of zinc layer has a direct impact on the quality of electroless nickel layer. [2] A uniform and smooth zinc layer certainly enhances the uniform growth of the subsequent electroless nickel deposit. [11] Many different methods have been investigated to provide better zinc deposit. For example, multiple zincate process, [11] control of bath chemistry, [2] and The influence of Al alloy substrate [6] etc. These methods will provide a uniform and smooth zinc deposit. However, most of this research has been focused on

industrial application. Although this research results in a more uniform layer with finer Zn grains, if we will gain the basic understanding of the nucleation behavior of zinc particles, we will control the morphology of zinc particle. Therefore, this study is focused on observation of the initial behavior and growth of zinc particles, which is hardly available in open papers.

In this paper, the zincating process is conducted by immersing the aluminum substrates into an alkaline zincating bath. The alkaline zincating bath containing ZnO and NaOH etch aluminum. Aluminum is dissolved into the solution as anodic reaction to release electrons for the Zn reduction as cathodic reaction. To increase the nucleation sites of zinc deposition, the zincating processes were conducted on Al alloy. [6] Also the zincating processes were conducted at high temperature to increase of growth rate.

Experimental Section

The P-type Si wafer was cleaned sequentially in trichloroethylene, acetone and methanol for 10 min in ultrasonic bath. Aluminum was deposited by DC magnetron sputtering method. All Substrates were initially cleaned in alkaline solution for 10 s followed by acidic cleansing for 10 s. The alkaline solution and the acidic solution were, respectively, 10% NaOH and 30 % nitric acid. The zincating process was conducted in 120 g/l NaOH, 4 g/l ZnO, 1 g/l NaNO₃ and 50 g/l C₄H₄NaO₆·4H₂O.

Section 1. Nucleation and Growth of zinc particles

The aluminum deposits were preparation by D.C magnetron sputter deposition using targets of 99.99% Al. Zincating process is carried out at room temperature by dipping the pretreated aluminum specimen into zincate solution.

Section 2. The increase of growth rate

The aluminum deposits were preparation by D.C magnetron sputter deposition using targets of 99.99% Al. Zincating process is carried out at 50 °C by dipping the pretreated aluminum specimen into zincate solution.

Section 3. The increase of nucleation sites

The Al-Cu-Si deposits were preparation by D.C magnetron sputter deposition using targets of Al (98.5%)-Cu (1%)-Si (0.5%). Zincating process is carried out at room temperature by dipping the pretreated Al alloy specimen into zincate solution.

Results and discussion

Nucleation behaviors of zinc particles

The aluminum substrate generally is formed a columnar structure with holes or boundaries by the magnetron sputtering system as shown in Figure 1. [5]

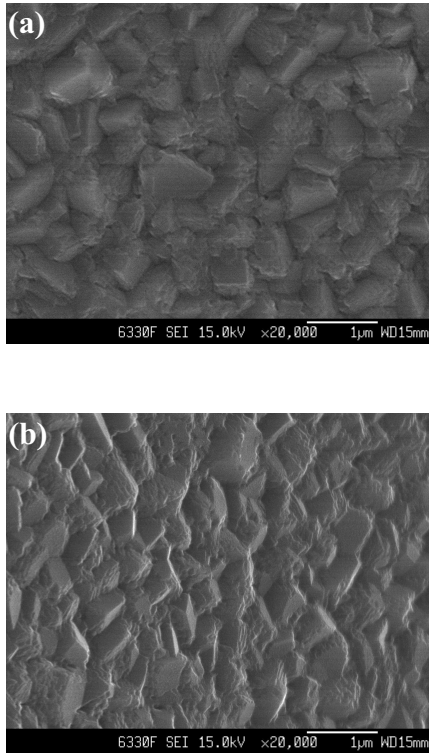


Figure 1. FE-SEM images of as-deposited Al specimen.
(a) Plan-view image, (b) tilted image.

When this aluminum with a columnar structure is exposed to the alkaline and acidic solution, the surface of the etched aluminum after pretreatment shows unevenness with holes (Figure 2).

In the Figure 2, when the aluminum is exposed to the alkaline zincating solution, the dissolution rate of each grain varies. Because of the difference in the binding energy of atoms between grain and boundary. Total energy involved in the binding energy and the subsequent dissolution of aluminum is faster for grain boundaries, which have the weak binding energy.

To investigate the an initial stages of zinc deposition on aluminum surface during zincating process, the surface morphologies of aluminum surface just after zincating process were observed by FE-SEM. Figure 3,4 shows the plane and tilted image of surface. Dissolution of the aluminum substrate continued along boundaries during the zincating treatment. However, zinc deposition occurs only on the film surface since zinc complex ion cannot reach the inside of holes [5].

The entrance into the holes of zinc particles is suppressed by exchange reaction. Leading to the dissolution of electronegative aluminum and deposition of a more electropositive zinc ion. The deep holes cannot be filled by zinc deposition, even though zincating time was increased to some degree as shown in Figure 5. As a result, after the

zincating treatment, zinc ions reduction occurred preferentially on convex part, corresponding to the peaks or edges of aluminum surface etched by zincating solution. Zinc particles form cluster, which were preferentially deposited at high surface energy area of aluminum surface. The above results indicate that zinc nucleation sites correlate to the surface roughness, [7] and electrochemical properties. [2,8]

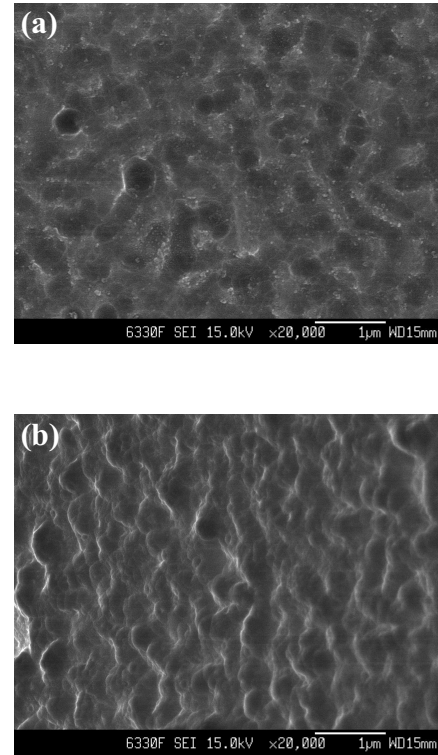


Figure 2. FE-SEM images of alkaline and acidic cleaned Al specimen. (a) Plan-view image, (b) tilted image.

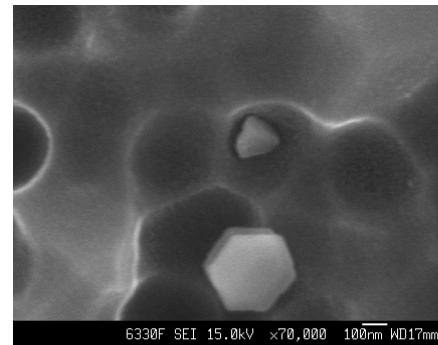


Figure 3. FE-SEM images of first zincated Al specimen for 10 s. (Tilted image with abnormal deposition behavior)

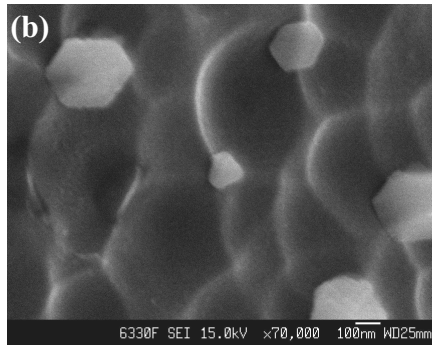
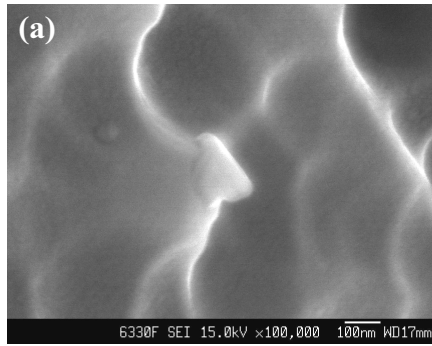


Figure 4.FE-SEM images of first zincated Al specimen after 1 second. (a) Titled image, (b) plan-view image.

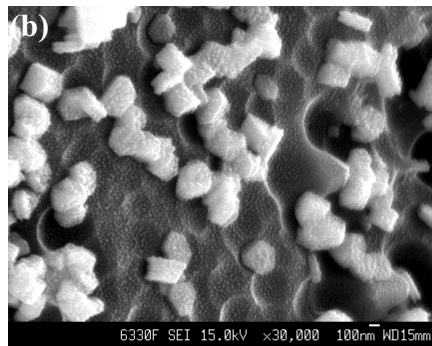
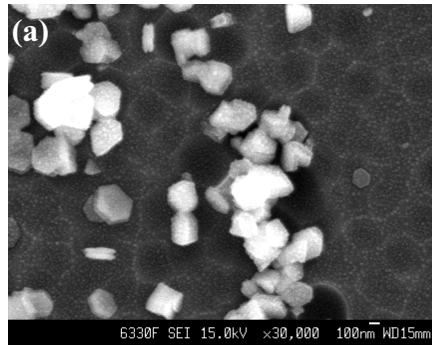


Figure 5. SEM Images of double zincated (10 s-10 s) specimen. (a) Plan-view image, (b) titled image.

Growth mode of zinc particles

Figure 6 shows the morphology of the stacking hexagonal platelets. At the initial growth stage (Figure 4b), Zinc particles form hexagonal platelet and grow with [0001] direction of hexagonal platelet as shown in Figure 6. Dissolution of

the aluminum substrate continues along boundaries. Therefore, the displacement reaction between anodic aluminum ions and cathodic zinc ions continues at a considerably fast rate, resulting in the formation of large zinc particles near the dissolution holes, as seen in Figure 4b. This shows that the morphology of hexagonal platelets which represents the basal texture. [9] The close packed planes, or the low index planes are known to be more resistance to dissolution because of the higher binding energy of surface atoms. [9] In hcp metals, The {0001} plane exhibits the best corrosion resistance [9]. In the Figure 6, The {0001} Plane has the most probability to stabilize thermodynamically; because this stack has the lowest energy state.

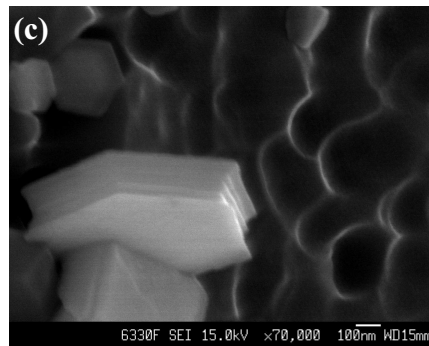
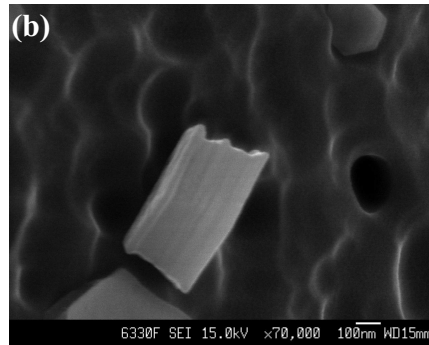
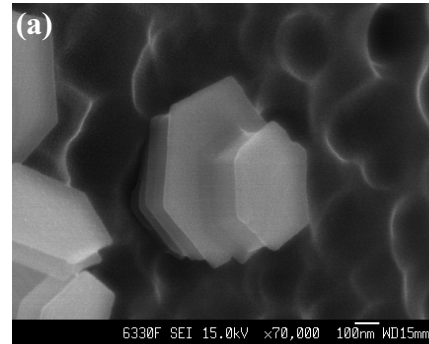


Figure 6. FE-SEM images of first zincated Al specimen for 10 s.

- (a) Titled image with normal stacking behavior,
- (b) Titled image with lateral stacking behavior,
- and (c) titled image with lateral stacking behavior.

Figure 7 show the SEM images that illustrate the microstructure of zinc growth deposited.

The zincate reaction occurs sporadically on the aluminum surface. The groups of hexagonal phase at isolated area were formed locally as islands (Figure 7a).

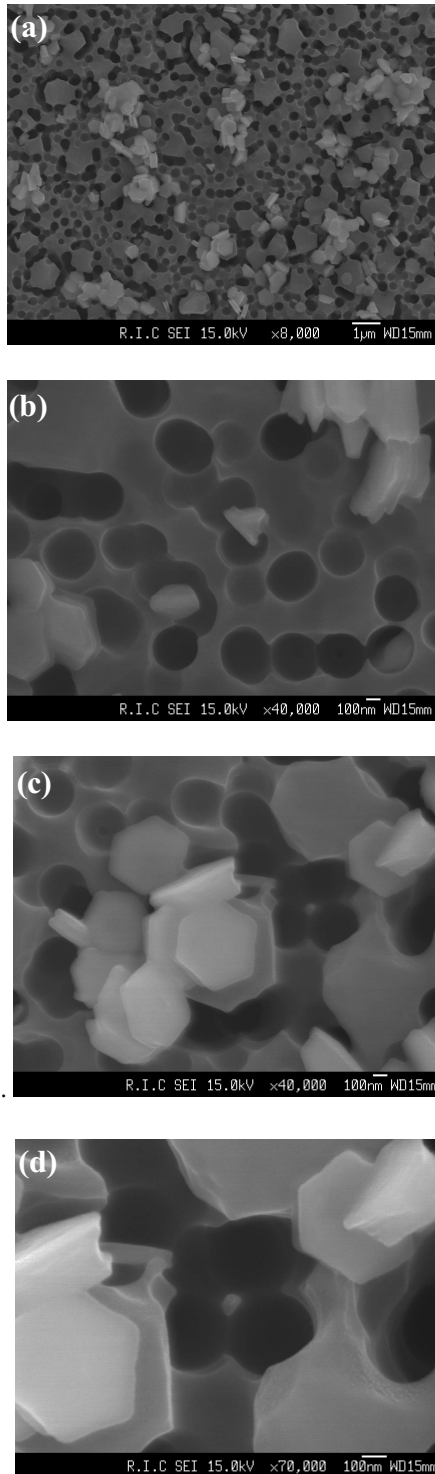


Figure 7. FE-SEM images of first zincated on same Al surface for 5 s. (a) Low magnification, (b) plan-view image with parent zinc particle, (c) plan-view image and (d) Plan-view image of parent zinc and groups of hexagonal platelets.

The increase of growth rate

When zincating process were conducted at 50°C, zinc particles grew with [1100]-oriented hexagonal structure and were appeared a starfish-like shape, due to thermally activated migration of boundary at high temperature (Figure 8).

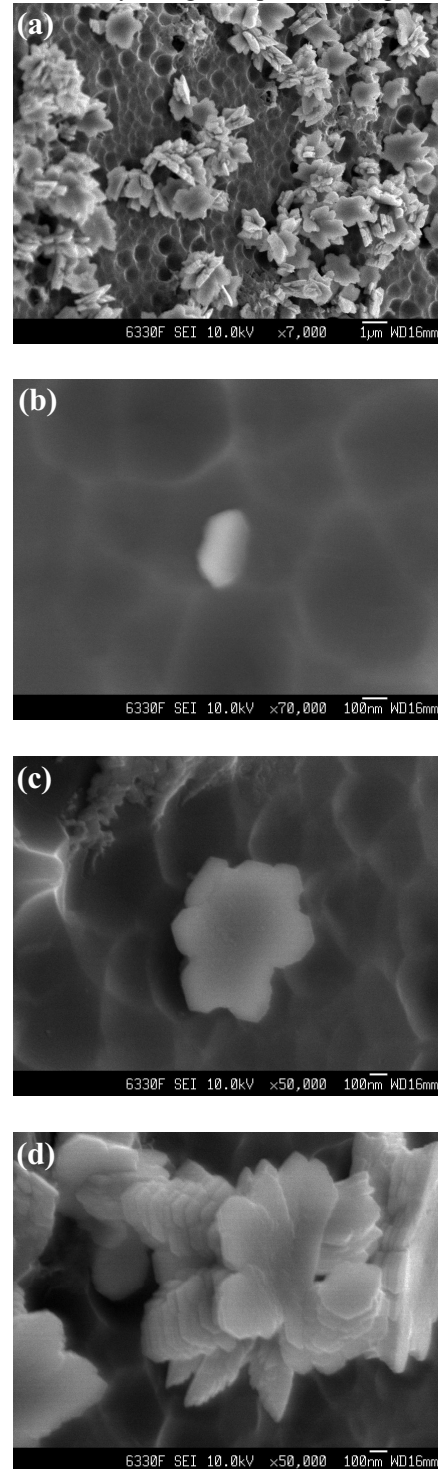


Figure 8. FE-SEM images of first zincated Al specimen for 10 s in 50°C zincate solution. (a) Low magnification, (b) titled image of hexagonal platelet, (c) titled image and (d) titled image with a starfish-like shape.

Comparison on Pure Al and Al alloy substrates

Figure 9 show SEI (secondary electron image) and BSE (back scattered electron) during zincating treatment for 1s on pure Al and Al-Cu-Si substrate.

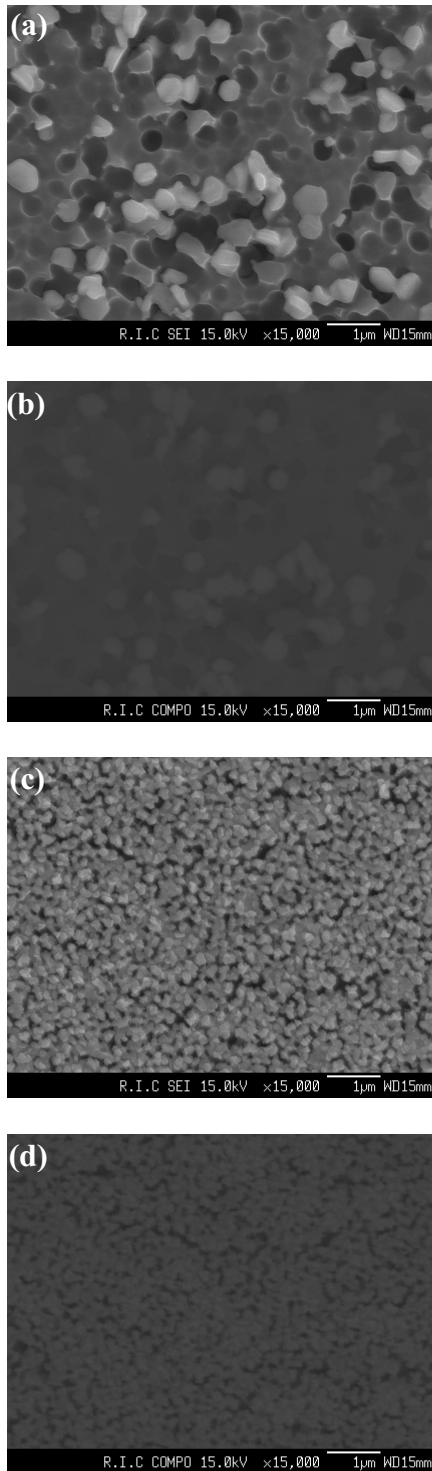


Figure 9. FE-SEM images of zincated pure Al substrate (a: SEI and b: BSE) and Al alloy substrate(c: SEI and d: BSE) for 5 s.

A comparison with Figure 9 shows that zinc particles on Al-Cu-Si substrate is considerably smaller than that on a pure Al substrate. In Figure 9a, most of zinc particles apparently covered sporadically. In Figure 9c, Al-Cu-Si substrate is fully covered by a thin layer of small zinc particles. This comparison indicates that the initial stage of zinc deposition on Al-Cu-Si substrate is faster than that on pure Al substrate. And the zinc nuclei on Al-Cu-Si substrate are more than that on pure Al substrate. These results indicate that zinc nucleation sites directly correlated to the intermetallic particles. Zinc nucleates preferentially on intermetallic precipitates in an Al matrix. [6]

The studies for the various influences of zinc deposition have been investigated by the three focus of (1) electrochemical properties of the cathode materials, (2) the effect ionic impurity in the electrolyte, and (3) the cohesion strength between the deposited metal and its substrate. [6]

Conclusion

During nucleation stage, the parent zinc is created on the peak or edge of Al surface. During the growth stage, zinc particles are migrated into parent zinc, and then hexagonal platelets formed. As a result, localized zinc islands were formed. At 50°C zincating process, zinc particles were appeared a starfish-like shape by the fast migration of zinc ions. Zinc nuclei on Al-Cu-Si substrate are more than that on pure Al substrate.

Acknowledgments

This work was supported by Center for Electronic Packaging Materials of Korea Science and Engineering Foundation.

References

1. J. H. Lau, *Flip Chip Technologies*, McGraw-Hill (New York, 1996), pp. 435-437
2. G. Qi, X. Chen, Z. Shao, Influence of Bath Chemistry on Zincate Morphology of Aluminum Bond Pad, *SEMICON Korea Technical Symposium 2001*, Session 8-3, pp. 1186-1190
3. Kwang-Lung Lin, Shiuh-Yuan Chang, The Morphologies and the chemical states of the Multiple Zincating Deposits on Al Pads of Si Chips, *Thin Solid Films* 288(1996) pp. 36-40.
4. C.J. Chen, K.L. Lin, Internal Stress And Adhesion of Amorphous Ni-Cu-P Alloys on Aluminum, *Thin Solid Films*, 370(2000) 106-113
5. Kazuhisa Azumi, Takuma Yugiri, Masahiro Seo, Shinji Fujimoto, Double Zincate Pretreatment of Sputter Deposited Al Film, *Journal of The Electrochemical Society*, 148(6) C433 C438 (2001)
6. Ping Gu, R. Pascual, M. Shikhanzadeh, S.Saimoto, J.D. Scott, The influence of Al substrate intermetallic precipitates on zinc electrodeposition, *Hydrometallurgy*, 37(1995) pp. 267-281

7. Mihalis Lazaridis, Qystein hov, Kostas Eleftheriadis, Heterogeneous nucleation on rough surfaces: implications to atmospheric aerosols, *Atmospheric Research*, 55(2000) pp. 103-113
8. C.J. Chen, K.L. Lin, A kinetic and electrochemical study of the zincate immersion process for aluminum, *Journal of Applied Electrochemistry*, 25(1995) pp. 659-666
9. H. Park, J. A. Szpunar, The role of texture and morphology in optimizing the corrosion resistance of zinc-based electrogalvanized coatings *Corrosion Science*, Vol.40, No.4/5, pp.525-545, 1998
10. Anhock. S, Ostmann. A., Aschenbrenner. R., Reichl. H, Qualification of the system electroless nickel bumps and PbSn5 for high temperature applications *Advanced Packaging Materials: Processes, Properties and Interfaces, 2000. Proceedings. International Symposium on 2000*
11. Chung-Daw Young and Jenq-Gong Duh, Adhesion Strength and Microstructural Evaluation in Electroless Ni-P Metallized AlN Substrates, *IEEE Transactions on Components, Packaging, and Manufacturing Technology*, Part A.vol.20, No. 3. September 1997

Fundamental Aspects in Bumping and Via Filling Electrodeposition

Kazuo Kondo

Dept. of Applied Chemistry, University of Okayama

3-1-1 Tshima-Naka, Okayama 700-0082, Japan

kkondo@cc.okayama-u.ac.jp

Abstract

Foundamental aspects in bumping and via filling will be addressed. A detailed mechanism of copper via filling will be emphasised. Copper Damascene via bottom accelerating additives was investigated by patterned cathode of cathode only at via bottom. With SPS in addition to Cl, PEG and JGB, the current of via bottom cathode increases. This current also increases with an increase in SPS concentration. This accelerating effect of SPS was found with typical combination of four additives (Cl+PEG+JGB+SPS) used for via filling. The current increases with an increase in aspect ratios of patterned cathode. With higher aspect ratio of deeper via, the via bottom accelerating substance must be accumulated at via bottom. This substance is related to SPS. Form the cross section observation of deposit thickness, this via bottom accelerating substance must form during electrolysis. This accumulates at via bottom of deeper via during electrolysis. SPS decomposes into monomer by electrolysis and this may accumulates and accelerates the via bottom current.

Introduction

Bumping and via filling electrodeposition became one of the most important process in recent development of electronics packaging. Especially, copper via filling has been intensively developed for damascene, build up PCB and three dimensional packaging. Micro bumping has been developed for higher pitch LCD interconnection, wafer level CSP and three dimensional packaging (Fig.1).

I started research on bumping when I was in industry since I was involved in the development of bumped type anisotropic conductive film (1). After moving to University, numerical computation of fluid dynamics within the bump cavity has been intensively studied at the diffusion controlled region. Numerical computations and experimental results coincidence have been examined for bumping with high Peclet numbers, photoresist angles, deep cavity, deep cavity for wafer level CSP (2-5).

The details of copper via filling mechanism (6,7) — inhibition and acceleration effects by additives, will be discussed in this proceeding.

Experimental

Table 1 shows the bath composition. The basic bath consists of CuSO_4 and H_2SO_4 of $0.6 \times 10^3 \text{ mol/m}^3$ and $1.85 \times 10^3 \text{ mol/m}^3$, respectively. Additives are Cl, PEG of 7500 molecular weight and JGB, whose concentrations are shown in Table 1. The baths were used for experiment more than one hour after the bath preparation.

The current-voltage curves were measured with R.D.E. with 12 mm in diameter. With potentiostatic electrolysis for the range of 100 to -400 mV vs. 3.33 mol/L KCl-AgCl, currents drop to constant value with less than three minutes.

Accordingly, all the currents were measured after three minutes from the starting of electrolysis. The R.D.E. was rotated with rotation speed of 150, 500 and 1500 r.p.m..

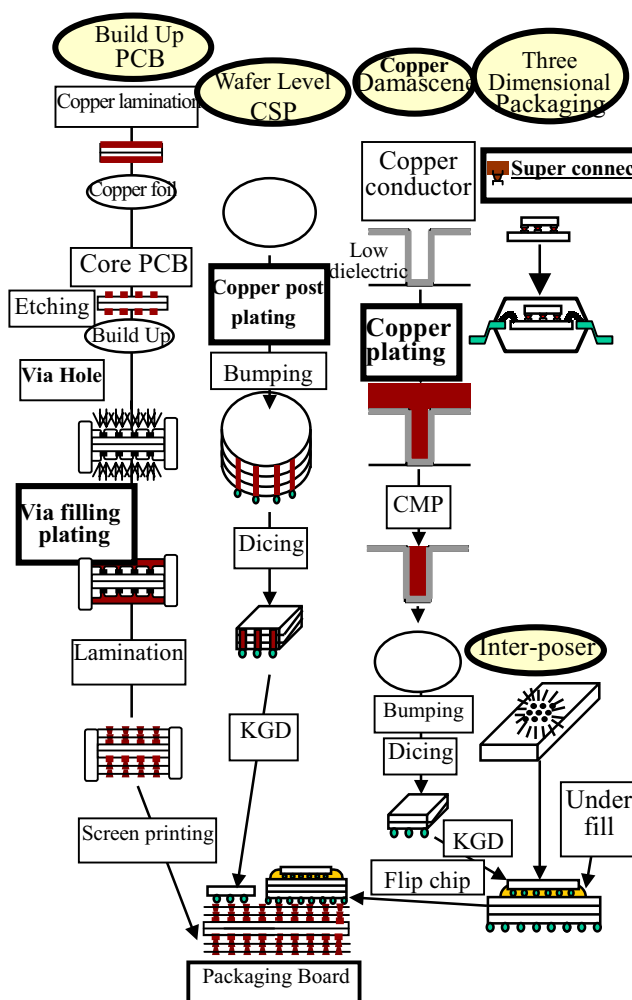


Fig.1 Recent electronics packaging process.

The patterned cathodes were prepared as follows. We formed $30 \mu\text{m}$ width and 10, 30 and $100 \mu\text{m}$ resist height pattern on copper foil. The photo resist of THB-430N (JSR Co.) was used. For 10 and $30 \mu\text{m}$ resist heights, the patterns were formed by photo lithography. $100 \mu\text{m}$ height resist was patterned by Excimer (KRF) laser with energy density of 1.0 Joul/cm^2 . The pattern has ten lines of 16 mm length with $30 \mu\text{m}$ width of 1.0 mm pitch. These photo resist patterns were attached to the rotating disk electrode (R.D.E.). The electrodeposits were prepared by constant voltage electrolysis of -200 mV vs. 3.33 mol/L KCl-AgCl without rotating the R.D.E..

Table 1 Bath composition.

Basic bath		
CuSO ₄ ·5H ₂ O		0.6 mol/L
H ₂ SO ₄		1.85 mol/L
Additive		
NaCl		100 ppm
PEG	Polyethylene glycol	400 ppm
JGB	Janus GreenB	10 ppm
SPS	Bis(3-sulfopropyl) disulfide	1, 5, 10, 20 ppm

The 30 μm width and 30 μm height resist was used for the pattern to observe the deposits cross sections. The pattern was already shown in reference 7. The electrodeposits were prepared by -300 mV vs. 3.33 mol/L KCl-AgCl without rotating the R.D.E.. 100, 200 and 400 C were applied. The deposits were then imbedded into the epoxy resin and cut and abrasive to obtain the cross sections. These cross sections were observed by optical microscopy.

Results

Current-Voltage Curves with Additives

Fig.2 is the current-voltage curves with different additives of without additive, Cl+PEG+SPS, Cl+PEG+JGB and Cl+PEG+JGB+SPS. The dotted curve is without additive.

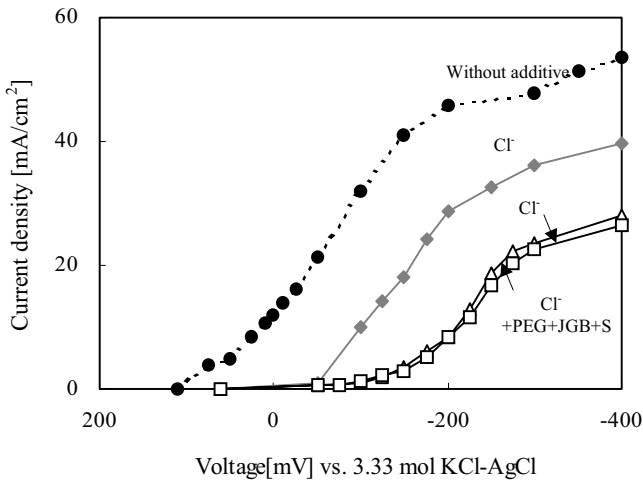


Fig.2 Effect of super-filling additives on current-voltage curves

With adding PEG and Cl, all curves shift to the cathodic side. This shift in cathodic side will be called as an inhibition effect by additives. With SPS in addition to PEG and Cl, the current increases if compared to Cl+PEG+JGB and Cl+PEG+JGB+SPS. This is due to the depolarizing effect of SPS. This depolarizing effect will be called as an acceleration effect by additives.

With SPS in addition to PEG, Cl and JGB, which is typical combination of four additives used for super via filling, however, the current does not increase. The curves with Cl+PEG+JGB+SPS and Cl+PEG+JGB are almost identical. SPS, in this case, does not seem to show the depolarizing

effect. These current-voltage curves correspond to J.Kelly's result(2,3,4).

Inhibition Effect by Additives

Fig.3(a)(b) is the current-voltage curves with different rotation speed of R.D.E. of 150, 500 and 1500 r.p.m.. The additives are Cl, PEG and JGB. With Cl and PEG of (a), current voltage curves does not shift with the rotation speed of R.D.E. With JGB in addition to Cl and PEG of (b), the curves shift to the cathodic side with an increase in rotation speed of R.D.E. such as 500 and 1500 r.p.m.. This shift in cathodic side with rotation speed means that the additives become diffusion control. Inhibition effect increases with rotation speed of R.D.E..

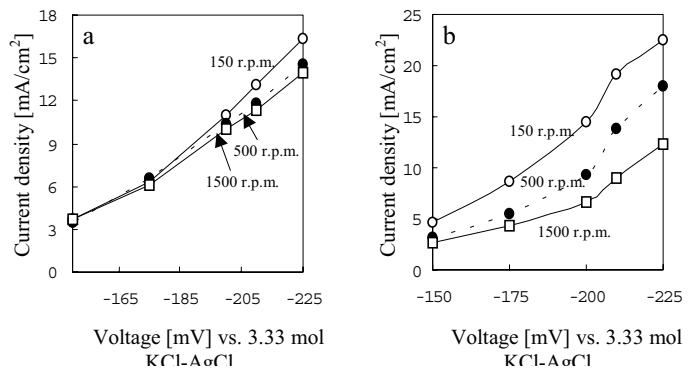


Fig.3 Effect of rotating disk speed on current-voltage curves with different additives. Additives are a) Cl and PEG, b) Cl, PEG and JGB

The adsorption of PEG molecules of about 30 nm in diameter causes this inhibition effect(7,8). The PEG molecules preferentially adsorb at the side wall of macro steps of copper electrodeposit and inhibit the lateral growth of the macro steps. Because of JGB, the PEG molecules become diffusion control. At the via outside, many PEG molecules are absorbed. Since via bottom has longer diffusion length than via outside, almost no PEG molecules can be observed at via bottom. This causes inhibition effect at the via outside and the electrodeposit preferentially fill the via bottom. This is one aspect of super via filling mechanism and this mechanism is based on the inhibition effect. Details of this diffusion control PEG molecules have already been discussed in references 7 and 8 with FESEM observations.

Acceleration Effect by Additives

We used patterned cathode of cathode only at via bottom in order to find out the acceleration effect(See Fig.4(b)). The current-voltage curves on conventional flat plate cathode have already been reported in Fig.2. Fig.4 shows a comparison of additive effect on current-voltage curves between this patterned cathode(b) and flat plate cathode(a). The additives are Cl+PEG+SPS, Cl+PEG+JGB and Cl+PEG+JGB+SPS. As have already been shown in Fig.2, the current-voltage curves with Cl+PEG+JGB and Cl+PEG+JGB+SPS are almost identical for the flat plate cathode(Fig.4(a)). With patterned cathode, these current-voltage curves are different(Fig.4(b); See white arrow). The current increases with Cl+PEG+JGB+SPS

if compared to Cl+PEG+JGB. This is because of patterned cathode. With patterned cathode, we succeeded to find the depolarizing effect of SPS with typical combination of four additives used for super via filling.

Fig.5 shows the current-voltage curves of patterned cathode with additives of Cl+PEG+JGB+SPS. The SPS concentrations have been increased from 1, 5, 10 to 20 ppm. The current increases with an increase in SPS concentration. We can conclude that SPS has depolarizing effect even with

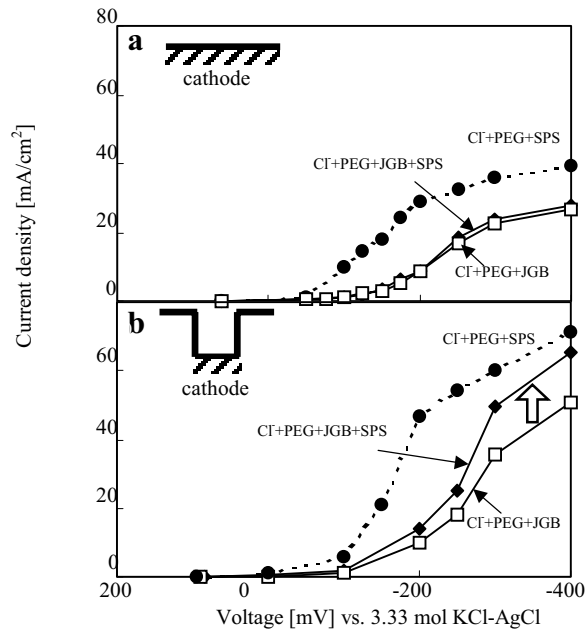


Fig.4 Current-voltage curves of flat plate cathode and patterned cathode. a) Flat plate cathode, b) Patterned cathode of cathode only at via bottom.

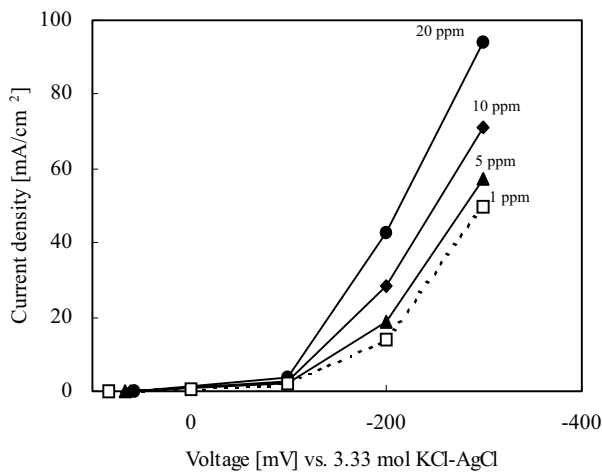


Fig.5 Current-voltage curves with different SPS concentration. Additives are Cl+PEG+JGB+SPS.

four additives of super via filling.

Fig.6 shows the current-voltage curves of different aspect ratios patterned cathodes with additives of Cl+PEG+JGB+SPS. The aspect ratios are 0.33, 1.00 and 3.33. Cathode width is fixed as 30 μm and the resist height has been changed as 10, 30 and 100 μm . The SPS concentrations are 10 and 20 ppm.

The current increases with an increase in aspect ratios of patterned cathode. The current increases with higher aspect ratio both for 10 and 20 ppm SPS concentrations.

Since the current increases with an increase in SPS

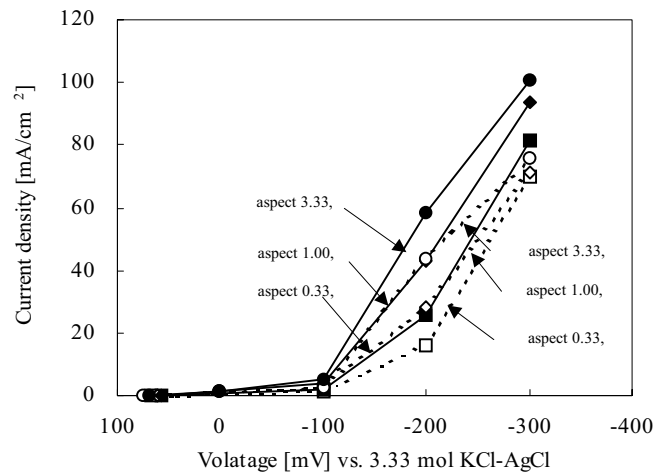


Fig.6 Effect of aspect ratio of current-voltage curves. Additives are Cl+PEG+JGB+SPS.

concentrations (Fig.5), a substance, which is related to SPS, accelerates the current of via bottom cathodes. This substance remains at via bottom since the current increases with deeper via of higher aspect ratios. This substance escapes easily from via bottom with lower aspect ratio of 0.33. The substance remains at via bottom and this accelerates the current at via bottom cathode of higher aspect ratio of 3.33.

Fig.7 is the cross section of via filling electrodeposition. The via has an aspect ratio of 1.0 of 30 μm bottom length and 30 μm resist height. Typical combination of four additives, Cl+PEG+JGB+SPS, have been used. The coulomb number has been changed from 100 C(initial stage), 200 C(middle stage) and 400 C(final stage). The lower white portion is the 30 μm in thickness copper foil and via is on the center of the copper foil. The 30 μm in thickness photo resists are on both

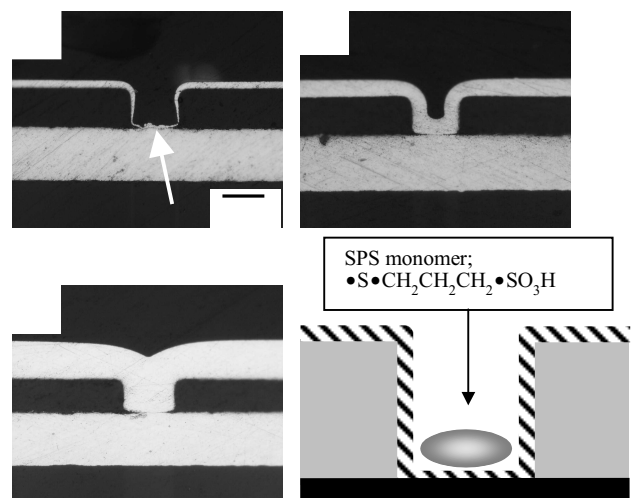


Fig.7 Cross sectional view of electrodeposit into via. a) 100 C, b) 200 C, c) 400 C, d) schematic illustration of SPS monomer.

The Effect of Roughness and Pattern of the Core Material to Adhesion in Making Build-up Layers

Paavo Jalonen*, Aulis Tuominen**

Pori School of Technology and Economics

Tampere University of Technology

Turku School of Economics and Business Administration

*email:Paavo.Jalonen@pori.tut.fi, ** Aulis.Tuominen@pori.tut.fi

Pohjoisranta 11

P.O.BOX 300

28101 PORI

Abstract

In very fine-line printed circuit board applications the problem of adhesion of the copper lines on the substrate material has been essential. When, in the future, the line width and spacing will be down less than 30 μm , very thin layers for etching the initial tracks are used. To get thin layers of metal, we used sputtering in seeding. There are several metals and combination possibilities for sputtering. In previous tests we have noticed that sputtered chromium gives a very good adhesion to copper in epoxy reinforced core laminat when the roughness of the laminat is R_a 0,6 μm and R_z 6,0 μm . However, when the surface of the substrate is too shiny (R_a 0,2 μm R_z 2 μm), not even chromium gives a proper adhesion. In order to get a good additive copper layer, it is recommended also to sputter a copper layer on the chromium and after that to grow, by an additive method, a thicker layer of copper on the laminat. In this paper we have studied the surface roughness of the substrate material and tested the adhesion strength of the metal layer on those surfaces. It has been shown that the surface must be even to be able to create fine lines, but if the surface is too shiny, an acceptable adhesion is not achieved.

Introduction

Adhesion to smooth surfaces is frequently insufficient, and mechanical roughening or chemical treatment of the adhered surface is often utilized prior to adhesive application. A novel roughening is achieved by molding the resin against the faying surface of the copper foil and subsequently etching the copper away. Other procedures are to use molten alkali etch of an epoxy surface [1].

As component packing densities increase, finer line widths and spaces as well as multilayer conductors are employed to interconnect circuits and there is an increasing need to safeguard conductor integrity and the insulation resistance between conductors. A typical damp heat stress condition of 85°C/ 85%R.H. for 700 hours has been employed to evaluate the reliability of conductors over 20 years. One method is immersion in NaCl at 100°C for 6 hours and drying, which has been found to give good correlation with exposure to 85°C/85%R.H. for 2000 hours [2].

In the fine-line (fine-line width is defined to be 0.10mm or less) fabrication surface treatment appears several times

which indicates that proper copper surface treatment is of paramount importance for good adhesion of etch resists as well as plated metal deposit [3]. Often used pumice treatment yields denrite matt finished surface, which provides not only maximum adhesion of resist to copper but at the same time, prevents exposure light from reflecting on the copper surface and blurring the fine-line conductor image. Surface depressions such as dents, pits, deep scratches and textured laminate surfaces may create "interfacial voids" i.e. tiny pocket of air trapped between the copper foil and the dry film resist during lamination. The situation is better by using the electrodeposited photoresist instead of the dry film. The air pockets are detrimental to fine line pattern formation because a portion of film may lift off, allowing etching or plating solution to creep in between surface and film.

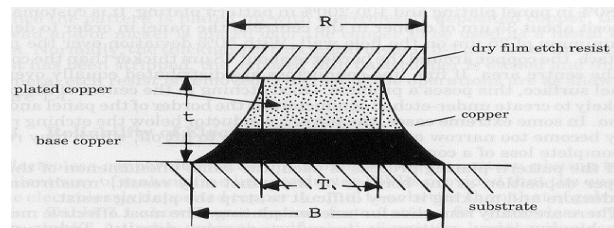


Figure 1. Etched line profile definition (panel-plating)

Etch factor = $2t/(B-T)$, in most cases, ranges from 2,5-3,5 depending on the thickness of copper to be etched, the etchants used, etching conditions, etching equipment and conductor width. R/B is defined as 1.

For high-speed applications, PWBs with controlled impedance are needed. When the clock rate has approached GHz, the signal attenuation will become mainly resistive because of the skin effect. At this point, the shape and resistivity of the conductor becomes very important. If the shape of the conductor is such that T/B becomes too small, not only does the resistance of the conductor become excessive, but impedance also begins to be affected[3].

Plasma enhanced chemical vapor deposition (PECVD) PWBs have been used for producing seeding layers for high-density interconnections. By using the PECVD-method and a seeding layer thickness of the metal approximately 10 nm, very narrow track lines like 15 micron have been generated on an epoxy resin surface by a full additive method [4]. The adhesion values from peel tests were then 10-18 N/cm.

Vacuum evaporation and sputtering are more commonly used techniques due to their maturity and availability of equipment. Titanium and chromium are the two most common adhesion enhancing metals used as a bond or glue

layer for conductor metals such as copper, silver and gold, which by themselves often do not bond well to most nonmetal surfaces [5]. To make thin-films structures and to enhance the adhesion of copper to polyimide as well as to prevent its interaction with polyimide, the copper wiring is sandwiched between two thin layers of Cr. By using sputtering and semi-additive copper Shimomoto etc. have developed very narrow lines using a special base material [10]. According to them, to obtain good adhesion and to form a micro-anchor to laminate they treated surfaces with a potassium permanganate. As adhesion layer they used Ti, TiW and Cr.

The basic adhesion is interfacial bond strength, which depends on the interfacial properties or interaction (electrostatic, chemical, van der Waals) and mechanical interlocking [11]. A good peel strength of the metal (chromium) to polymer (polyimide) is about 76-90 g/mm [6]. The value for copper clad laminate is usually mentioned in data sheets to be 1,3-1,6 kp/cm (thickness 17 μm).

Because sputtering is impractical due to its low throughput, we began to develop a sputtering method to be used in volume. Tests have been made to help in selecting the best molecular metallic seeding layer for electroplating by using sputtered metals in a particular printed circuit board manufacturing process. The adhesion of different sputtered metals to laminate have been measured in a continuous manufacturing process as a dry process, in which there are no chemicals to handle, no rinse water to be treated and no spent baths to treat. Plasma etching and sputtering are dry processes which have been used to desmearing, etchbacking and seeding. One big advantage of the plasma technique is that all the different laminate material types can be treated, although each may require a unique cycle time [7]. To guarantee the reliability of the high density PCB in over-all production the adhesions of the base materials may be one of the most important issues [8].

Size reduction becomes very difficult when the quality of the substrates must be improved or at least maintained at the same level as in larger devices. In consumer products the use of organic printed wiring boards (PWB) instead of ceramic is preferred. In direct chip attachment (DCA) processes many factors, like the coefficients of thermal expansion, the adhesion to solder resists, PWB planarity, etc. have a great impact on the final quality [7]. In very narrow lines and space widths, the accuracy of the whole printed circuit board manufacturing process will become very critical. It is preferred to use thin metal layer, which can be etched easily and after etching, the copper can be grown up to the decided thickness in so called build-up process. It is important to have thin and even photo resist, without any pinholes. High demands are also put on the photo resist used in exposure process. In conventional PWB process dry film photo resist is generally used, since it is simple to apply on the PWB laminates. The exposures process itself is also critical and must be done in a clean room and by using collimated light. Material selection is one of the most critical factors, especially the smoothness of the laminate where lines are produced. If the surface of the laminate is too rough, a tiny line can be broken or too short compared to the neighboring lines [12]. On the other hand, the adhesion of initial metal also depends on the roughness of the surface, and an appropriate peel strength of the lines must be guaranteed. It has been shown that by using sputtered interface metallic layers an acceptable peel

strength can be achieved. Especially when the interface metal is chromium the peel strength is usually good.

In this study we measure the peel strength of numerous metal seeding layers on differently treated FR-4 surfaces. Chemical and mechanical treatments are used for roughening epoxy surfaces. These are the low cost methods. At the same time we made tests to compare the suitability of three different photo resist to fine line technology and characterize the effect of roughness on accurate of the lines starting from 1 micron. The objective of these tests was to find out the best seeding layer(s) and roughness of laminat(s) suitable for additive copper, used, to measure peel strength forces.

Although a special adhesion layer on the board has worked quite well, there are a number of underlying objections to this approach. Because the adhesive layer has a poor dielectric performance, an accurate impedance control of the product cannot be reached and if we use reinforced laminate and the adhesion material is not present, the material tends to have different expansions in the x-, y- and z-directions.

1. Experimental set up

1.1.Sputter deposition

Sputtering, formulated in 1852 by Grove [9], is a process that can deposit any material on any substrate. It takes place in a vacuum. It is a physical process and is referred to as physical vapor deposition (PVD).

The target is a solid, grounded slab of the desired film material. In our tests we used a magnetron-sputtering system (Fig.2), in the machine that had been developed for this purpose. The distance used between the target and the laminate was exceptionally short, only 20 mm. The magnets capture and/or confine the electrons at the front of the target and are more efficient for increased deposition rates. The laminate moved vertically up and down during the sputtering. Thus the deposit was uniform all over the surface. The sputtering time was 20-40 sec. The thickness of the sputtered film was 0.3-1.0 μm .

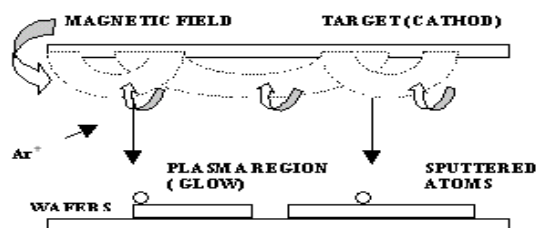


Figure 2. Principle of magnetron sputtering

A di-functional epoxy-reinforced Fr-4 base material was used in all specimens (T_g 140°C). The pieces of laminate were without copper, and five kinds of pretreatment were used. The first step was solvent cleaning in an ultrasonic cleaner using 2-propanol. After that a part was brushed mechanically using a conventional brushing machine, and a part was both brushed and etched in concentrated sulfuric acid (92-95%) in room temperature, Table 1. The roughness of these all samples is given in Table 2.

Some samples were coated with an epoxy surface, thickness 40 μm , before the chromium sputtering to see the effect of very fine smoothness to adhesion. In Table 2. can be seen

the used smoothness values Ra and Rz and a mathematical descriptions of the values in Figure 3.

Table 1. Different types of specimens

TARGET /PROCESS	1	2	3	4	5
Copper- Silver	X	X	X	X	X
Silver	X	X	X	X	X
Chromium-Nickel	X	X		X	
Acid proof Stainless Steel	X	X		X	
Titanium	X	X		X	
Chromium	X				
Copper	X				

Process 1: ultrasonic cleaning (USC) in iso-propanol
 2: USC + brushing
 3: USC + conc. sulf.acid
 4: USC + brushing + conc.sulf.acid
 5: USC + brushing + conc.sulf.acid + deacidification

Table 2. Smoothness values of samples

Ra and Rz values of the laminate samples in μm			
After brushing		Epoxy surface	
Ra	Rz	Ra	Rz
0,80	6,05	0,23	2,05

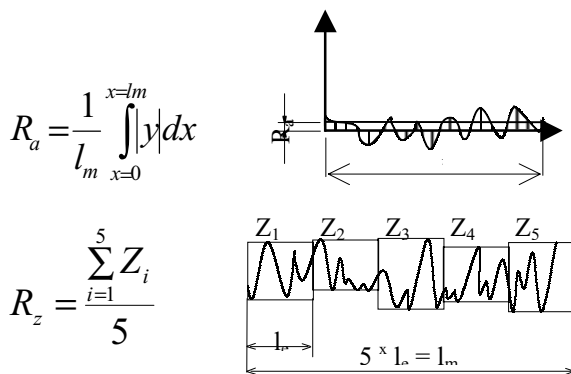


Figure 3. Mathematical description of values Ra and Rz

The specimens were sputtered in-line using different targets and were immediately electroplated in a standard acid coppersulphate plating bath without pretreatment. After copper growing, a circuit-imaging process was applied using a dry film photo-resist, and etching was done in an ammoniacal etch liquid. The rest of the sputtered chromium layers were stripped in an ammonium-cerium-nitrate liquid. The pulling strips were brushed and visually examined to observe the failure mode. A third of the sample was anneal heated in 105°C, 60 min (in Fig. 4. marked by the symbol "t"), and one third was treated in 170°C, 70 min under pressure. Finally the coupling units for peeling clamps were joined by a tin-lead paste.

1.2. Pattern

A total number of four roughnesses of the laminate surfaces was used. One of them was without any treatment and three

others were brushed in a brushing machine, having two brushing heads, the first head against feed direction, the second head with a feed direction, Table 3.

Table 3. Average roughness of the FR4 laminate samples in tests.

Sample/ Roughness	Rz	Ra
A	6.0	0.80
B	4.98	0.58
C	3.84	0.54
D	3.37	0.36

The roughness of the surfaces was analyzed by using Perthometer M4P. The chromium metal layer was sputtered on the 1 mm thick laminate. The chromium layer was coated with additive copper about 3 μm . This was done to distinguish better the fine resist lines on the shiny copper surface.

On this metal layer positive photo resists were applied to define the best combination for pattern and its surface roughness. Three different resists types were used, dry film (35 μm) spin resist (8-10 μm) and electro-deposited (ED) resist (15 μm).

The test patterns had several parallel lines, since this type of arrangement gives the best evidence, how well the gaps can be cleaned between the mask lines in development. In the exposure the glass mask was used and collimated light, having a wavelength about 380-450 nm. The exposure time for photo resists has characterized by Stouffer 21-step sensitivity guide. The development of the resist was done by using sodium carbonate, 1 %. Etching of the chrome was done by ammonium cerium (iv) nitrate liquid. The etching time is only few ten seconds, when the chrome layer is thin. The line width used in the test varied from 1 μm up to 100 μm .

2. Tests and results

2.1. Adhesion tests

The peel strength or copper-bond strengths are specified in IPC-4101 (MIL-P-13949) and by NEMA standards. The study was made before the soldering operation. The rate of pulling was 5 mm/min and the minimum load of the force indicator was recorded. The track of the peeling strip, (thickness 20 μm), in all specimens was 3.18 mm (1/8inch). The pullings were done on an appropriate machine and in every case the test was made minimum five times for each type of specimen. The deviation of strength in the tested peeling strips is illustrated in Figure 4. There the average value of adhesion in each case can be seen.

1.2. The Effect of roughness to patterning.

The results were estimated by looking at how well the spaces between the lines were open after development. It was noted that a brush rougher than B (Table 3.) roughens the surface from the original value and a brush finer than D does not change the surface, because abrasion is too small. Application of photoresists was straight forward, with the ED-process being the simplest one. The dry photoresist was applied by the PWB manufacturer; other resists were applied by us. It was noted that the cleanliness of the surface in the ED-process is vitally important for getting a

smooth surface. The results showed the smoother the laminate's surface, the better the result in pattern. However, only slightly brushed surfaces did not give much better results than with the original, but the effect of brushing could be seen well only with the finest surface. It was also noted that thick, dry film is out of question, when very tight lines and spaces must be achieved. With spinning we also expected to get good results, but the spun photoresist had rather poor adhesion and narrow resist lines were easily detached from the metal surface during development. The best results were achieved using ED photoresist. Adhesion was very good and the resist was thin enough to make the lines under our 10 μm target and even less. The effect of surface roughness especially on the finest side also had a great impact on line width and accuracy in the developed photoresist. The smoother the surface, the better the resolution.

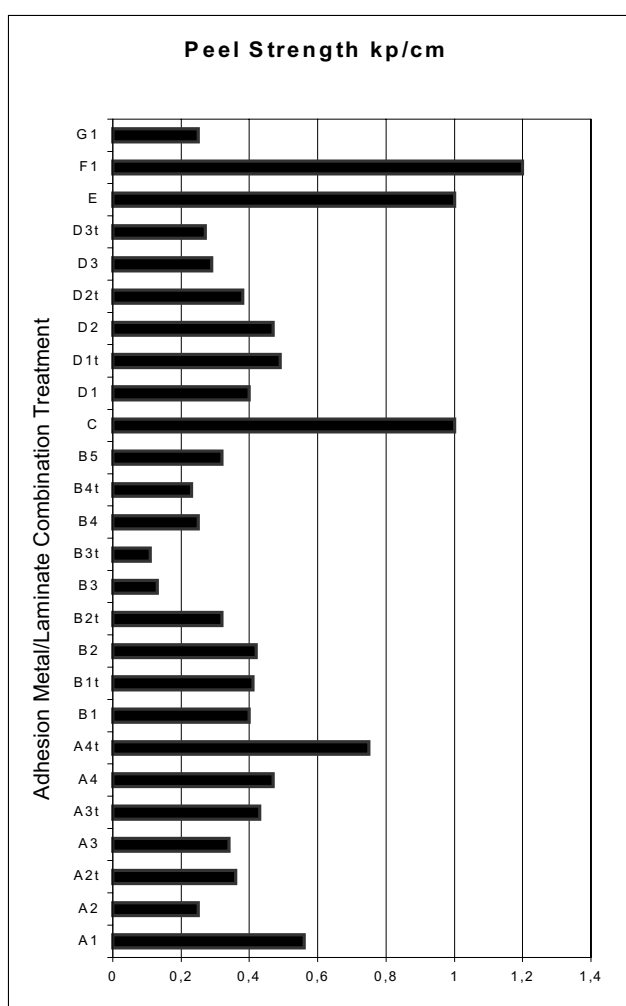


Figure 4. Peel Strength of electrolytic copper on different pretreated epoxy laminates using different metallic seeding layers

3. Discussion

Before the peel strength test we observed by visual inspection that in some strips delamination of silver occurred from the surfaces of the laminate. Delamination of copper on sputtered chromium occurred when the epoxy surface had a smoothness less than $R_a: 0.2 \mu\text{m}$ and $R_z: 2 \mu\text{m}$.

Both in the cases of titanium and chromium/nickel the peel-strengths between copper and the metallic layer were

smaller than the forces between seeding layers and laminate. Delamination occurred when the peel strengths were about 1 kp/cm. This depended on insufficient pretreatment of the titanium and chromium/nickel metal for plating before electrical copper plating. One way to produce slightly better adhesion of copper to titanium is to apply immersion copper from different solutions or to sputter some other metal over titanium [9].

Using the adhesion of a chromium seeding layer we measured values 1.2-1.6 kp/cm and they were found to be the best one. The values varied with the pulling distance. In all measurements the variation occurred at regular distances 6-7 times within 5 millimeters as we can see from figure 5. The variation depends on the glass fabrics of the laminate used.

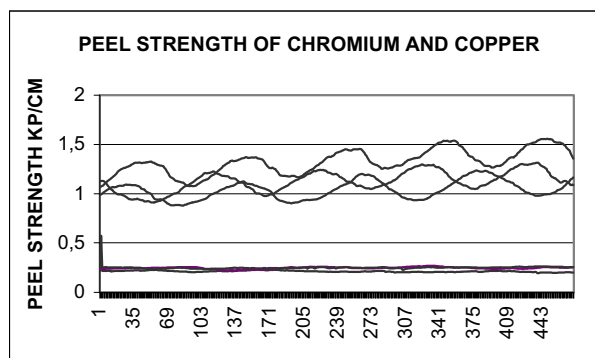


Figure 5. Peel Strength of sputtered chromium (upper) and copper (lower) seeding layers

The second best adhesions to the metallic layers and laminate were with titanium and with Cr-Ni. After these a good metallic layer seems to be Cu-Ag. Adhesions seem to increase in heating above the T_g -point as happens in the Cu-Ag case.

In these cases adhesions increased by more than double but are still not good enough. The inverted effect happened in pure silver and in acid-proof stainless steel in the first heating to 105°C, 1h. Oxidation of interface metals and diffusion between interface and base copper may be the most important reason for the failure. In some cases the treatment with sulfuric acid has increased the adhesion. The adhesion of the sputtered film to the laminate surface is also improved over the evaporation process. The higher energy of the arriving atoms makes the adhesion better.

By using ED method the photo resist layer will become very thin, being thus easy to develop. The thickness of the ED resist depends on the time, when high voltage to the substrate is applied. Moreover, the ED process itself guarantees that no pinholes exist, since the material continues to grow as far as there are any conductive surfaces having applied tension and will terminate after the isolation of the resist will become good enough to prevent ED process to continue.

3. Conclusion

The best adhesion ratios of seeding layers were with chromium (over 1.6 kp/cm), chromium-nickel and titanium. Acid-proof stainless steel and copper-silver indicated their suitability in follow-up tests. Low temperature heat treatment had no measurable results. These measurements

were made using roughness Ra 0.6 and Rz 6.0 microns. On "mirror like" surfaces, Ra 0,2 micron, delamination took place.

In the patterning the effect of three different photoresists and four laminate surfaces on fine line resolution were characterized. It has been noted that the best results were achieved using ED-photoresist. The resist changed from slightly to thick, when using a 15 s process time. A shorter time is recommended. The roughness of laminate has a great impact on fine line resolution, but it can be seen that the adhesion of seeding layer is better using rougher surfaces. However, with the existing brushing method it is possible to go down to our targeted 10 μm in both line and spacing.

The test showed that a proper combination of the surface roughness and the patterning have a great impact on the quality when making very thin tracks.

References

- [1]. H. L. Rhodenizer, J. J. Grundwald, W. P. Inness. "Additive Process Used for Printed-Circuit Boards" U.S.patent No. 3,666,549,1972.
- [2]. F. N. Sinnadurai, Handbook of Microelectronics Packaging and Interconnection Technologies 1985.
- [3]. G.Herrman,K.A.Eegerer, Handbook of Printed Circuit Technology, EPL,1992.
- [4]. R. Schulz, E. Klusmann, J. Schulze, H. Meyer, Plasma Enhanced Chemical Vapor Deposition For the Production of High Density Interconnects, Second Workshop on Advances in Printed Circuit Board and Substrate Technologies, Berlin 1999.
- [5]. J. Zhang, J.W.Golz, M.Gorski, J.Schmitt, B. Halpern, Jet Vapor Deposition: A New, Low Cost Metallization Process. IMAPS, Pennsylvania 1997.
- [6]. R.R. et.al. Tummala, Microelectronics Packaging Handbook III, Chapman&Hall, New York, 1997.
- [7]. W. Jawitz Martin Printed Circuit Board Materials Handbook, McGraw-Hill,USA,1997.
- [8]. P. Jalonen, A. Tuominen, The Importance of Solder Resist Adhesion in Flip Chip Application, PCB Electronics, JCE, Nov., 1999.
- [9]. AJ. Aronson "Fundamentals of Sputtering" Microelectronics Manufacturing Grove and Testing, January 1987.
- [10]. T. Shimoto, K. Matsui, Y. Shimada, K. Utsumi, New High-Density Multilayer Technology on PCB, Electronic Component & Technology Conference, IEEE, 1998.
- [11]. K.L. Mittal, Edit. Adhesion Measurement of Thin Films, Thick Films and Bulk Coating, ASTM, 1978.
- [12]. P. Jalonen, A. Tuominen, The Effect of Core Material Surface Roughness on Line Accuracy using Electrodeposited Photoresist, EMAP, Hong Kong, 2000.